Current Chemistry Letters 12 (2023) 739–758

Contents lists available at GrowingScience

Current Chemistry Letters

homepage: www.GrowingScience.com

A review on Schiff base as colorimetric and fluorescence sensors for d-metal ions

V. Inbaraj[a] and Duraisamy Udhayakumari[a*]

[a]*Department of Chemistry, Rajalakshmi Engineering College, Chennai – 602105, India*

C H R O N I C L E

Article history:
Received December 25, 2022
Received in revised form
January 28, 2023
Accepted May 6, 2023
Available online
May 6, 2023

Keywords:
Schiff base
Fluorescent probe
d-metals
PET
ICT

A B S T R A C T

Most of the d-metals are familiar with their distinctive properties and their applications have been extended in vast industry fields. Though they are doing outstanding work in industries and help to boost the economy of dependence. The excess uptake of d-metals explores significant health issues, and detrimental effects on the environment, and corrodes the biological species. Fluorescent probes based on Schiff base chemical compounds give more accuracy, and low-level detection for metal ions in water, chemicals, and in biological cells through commendable and quick fluorescence signals. So, it empowers the successful detection of d-metals in terms of dissimilar fluorescence responses by probes in light of metals. Based on the recent research in the field of Schiff base-based fluorescent probes and interpretation on effects for binding like ON-OFF PET, ICT, CHEF, and CHEQ this imperative review is framed.

List of Abbreviations

AIEE – Aggregation-induced emission enhancement
CDs – Carbon dots
CH_3CN – acetonitrile
CH_3OH – Methanol
CHEF – Chelation-enhanced fluorescence
CORM-3 – Carbon monoxide-releasing molecule-3
DMF – Dimethylformamide
DMSO – Dimethyl sulfoxide
DN – Donor number
DNA – Deoxyribonucleic acid
DNH – Dinitrophynylhydrazine
DPA – dipicolylamine
EDTA – Ethylenediaminetetraacetic acid
ESI MS – Electrospray ionization mass spectrometry
ESIPT – Excited-state intramolecular charge transfer
FRET – Forster resonance energy transfer
GSH – Glutathione
H_2O – Water
HCl – Hydrochloric acid
Hcy – Homocysteine
ICT – Intramolecular charge transfer
LOD – Limits of detection
nM – Nanomolar
NMR – Nuclear magnetic resonance spectroscopy
PBS – Phosphate-buffered saline
PET – Photoinduced electron transfer
Ppb – Parts per billion
Ppt – parts per trillion
RGB – Red-Green-Blue
TFA – Trifluoroacetic acid
TLC – Thin layer chromatography
TNP – Trinitrophenol
TNT – Trinitrotoluene
µM – Micromolar

1. Introduction

There is an urgent call for active detection of harmful transition metal ions namely, Cr^{3+}, Fe^{3+}, Cu^{2+}, Zn^{2+}, Cd^{2+}, Co^{2+}, and Hg^{2+}due to their adverse effects in the environment. Further, environmental safety, pollution control, conservation of biodiversity, the safety of human life, and survival fitness has faced a kind of threat by the overwhelming presence of d-

* Corresponding author.
E-mail address udhaya.nit89@gmail.com (D. Udhayakumari)

doi: 10.5267/j.ccl.2023.5.001

metal ions. There is a mandate on keeping the range of these metals under the level directed by WHO, ICMR, and BIS in India[1-15]. Instead of going with some inaccurate, costly, long-duration for detection, that needs the aid of skilled personnel, low lifetime, and weaker detection limit, there is a great opening for Schiff base-based colorimetric and fluorescence sensors to detect the key elements in aqueous, chemical, and in living species. Schiff base probes contain a nitrogen atom and oxygen atoms analogy of an aldehyde (or) ketone in which the C=O group is replaced by the C=N-R group. Schiff base probes are used as pigments, catalysts, intermediates in organic synthesis, polymer stabilizers, dyes, biological activity, molecular memory storage, imaging systems, pharmaceutical, and agro-industrial chemistry[16-24]. In recent years, the investigation expanded on the design, synthesis, characterization, and applications of Schiff base probes in the field of molecular recognition, supramolecular chemistry, and metal coordination. Since the Schiff base derivatives contain nitrogen-oxygen-rich sites along with free electrons which is a sign of good ligands because they can be a very good receptor to accept the metal ions. However, the method of investigation to detect d-metal ions by Schiff base-based molecular moieties found an excellent method over weaker methods due to cost-effective, easy, transparent, and great selectivity detection and which are accounts of strong fluorescence enhancement and quenching, distinct color differences, and rehabilitation via crucial binding mechanisms such as PET (Photo-induced electron transfer), ICT (Intramolecular charge transfer), CHEF (Chelation-enhanced fluorescence), AIE (Aggregation induced emission), CHEQ (Chelation-enhancement quenching effect) in presence of electromagnetic radiation in UV-Visible wavelengths[25-35].

Investigation for the d-metal ions in real samples with a diverse group of mechanisms by Schiff base-based sensors is fascinating at present. Chen *et al*. reported a list of simple probes for lead, cadmium, and mercury ions detection[26], and Upadhyay *et al*. published a report based on developed colorimetric sensors for d-metals from the year 2003 to 2018[27]. Duraisamy Udhayakumari *et al*. reported an input upon Schiff base-based chemosensors for cell imaging applications[28] and Khan *et al* summarized recently fabricated Schiff base-based fluorescence sensors for various transition metals[29]. To the best of our knowledge, this is the first review established for a quick recap and intended over the developments of Schiff base-based fluorescent probes especially for industrially, biologically, and environmentally important d-block metal ions. This review listed out the simple Schiff base-based fluorescence probes which have been developed in the last few years.

2. Schiff base Fluorescent Probes for d-Metal ions

2.1 Fluorescence Probes for Chromium Ion (Cr^{3+})

Chromium is an essential and highly brittle trivalent heavy metal element with an atomic mass of 24, which is pretty prevalent for high corrosion resistance in nature. The chromium trivalent (Cr^{3+}) ion acts as a vital nutrient in the human body at the metabolic reaction of insulin, sugar, lipid, and carbohydrates, so it plays a major role in the good health of humans. One of the unavoidable metals in the production of stainless steel, various alloys making, pigments, and in leather processing since its high hardness and best corrosion resistance. The very minimum intake of this mineral through different diets can cause glucose intolerance, diabetes, and CVD in humans. Despite its essential need, there is always a life threat for humans and causes some environmental effects, when it has been overtaken. Hence, the recommended amount of chromium through daily dietary intake is 0.05 mgL^{-1} as per the recent proclamation of WHO[36-44].

Triphenylamine-Thiophenegroups coupled based on this, probe 1 was synthesized and used to measure the strength of Cr^{3+} in an aqueous medium[36]. The free fluorescent moiety showed very good emission in THF among other solvents at 530 nm. The additions of Cr^{3+} have brought a strong fluorescent emission 59 times higher than the fluorescence signal by the metal-free moiety. This would help us to rate the applicability of the above-said probe 1 for Cr^{3+}. The movement of an electron from donor to acceptor was limited completely by adding Cr^{3+} into the probe that inhibited the PET effect which has been noted on the other hand a Saxon blue color has also been noted in the result of complex formation this could be the reason for binding mechanism (**Fig. 1**). The selectivity of probe 1 was highly transparent towards Cr^{3+} ions and has no inference with other metal ions. The LOD was measured as $1.5x10^{-6}$ M for Cr^{3+} ions.

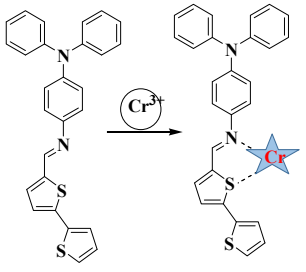

Fig.1. Structure of fluorescence probe1 with Cr^{3+}

Novel Schiff base-based fluorescence probe 2 was developed via a synthetic route for Cr^{3+} ions in polar aprotic acetonitrile (95/5%) by Chalmareli *et al*.[37] Further, it showed great affinity towards Cr^{3+} ions. Such affinity was demonstrated with the help of fluorescence spectral studies on the addition of Cr^{3+} ions to probe 2. The increasing

concentration of chromium ion in a solution of probe 2 exhibited an emission spectrum at 663 nm owing to an inhibition of the photo-induced electron transfer process during complex formation (**Fig. 2**). This helps to conclude that probe 2 acts as an effective sensor for Cr^{3+} ions. The calculated detection limit was 1.3×10^{-7}mol/L by probe 2.

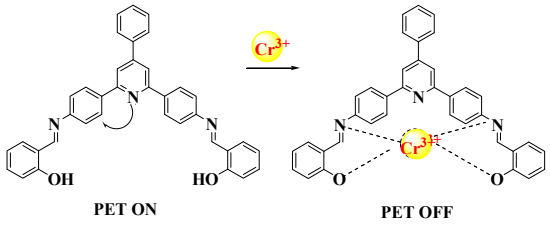

Fig. 2. Structure of probe 2 and metal binding mechanism

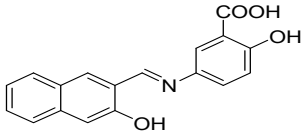

Fig. 3. Chemical Structure of Probe 3

Zhang *et al*. developed a fluorescent probe 3 for Cr^{3+} as a multiple metal ion sensing system based on the learning from the experience of previous studies[38]. They have enabled the inclusion of the Schiff base compound to improve the effective detection of probe 3 for Cr^{3+}ions. During spectral studies, a clear color change on the delivery of Cr^{3+} ion into probe 3 was noted within the naked eye. Additionally, the UV-visible spectral studies have also been conducted by adding metal ions into probe 3, result has proved the relation between Cr^{3+} and fabricated probe 3 by decreased absorption beak (<447nm) from the base beak of probe 3. Further, the binding mechanism was predicted based on the following measures: proton peak shifting in the imine group, missed out intramolecular hydrogen bond in the naphthalene ring, and involvement of an oxygen atom from a carboxylic acid group of the benzene ring in probe 3. Hence, it showed the detection limit was 3.37×10^{-7} M. The binding constant was found to be 2.06×10^{6}, for Cr^{3+}, according to the Benesi Hildebrand equation (**Fig. 3**).

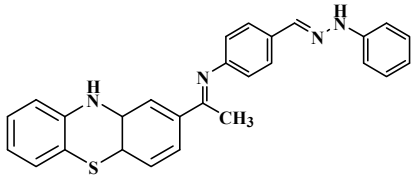

Fig. 4. Chemical structure of probe 4

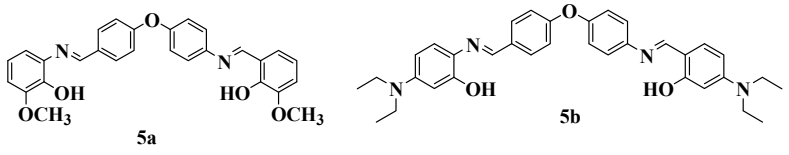

Fig. 5. Chemical structure of probes5a and 5b

Simple organic molecule structure designed by Vijayakumar and his crew members for the detection of Cr^{3+} ions actively in an aqueous medium[39]. The color of fabricated probe 4 was modified when it was treated with Cr^{3+}ions. The addition of Cr^{3+} ions into probe 4 brought an intense fluorescence emission peak at 428 nm. On the other hand, the binding mechanism of probe 4 to Cr^{3+} ions have found that the restriction on free-electron transfers from -C=N to -NH group (quenched PET process). It appeared that probe 4 responded well to the Cr^{3+} ion that confirmed the selectivity towards probe 4 (**Fig. 4**). Two-salicyl aldimine derivatives converted into two sets of fluorescent Probes 5a, and 5b for Cr^{3+} ions by Kolcu *et al*.[40] An intense emission at 530 nm is owed to the ICT process in probe 5a. Found it has certainly changed by the addition of Cr^{3+} ion and emerged an emission band at 508nm by causing a blocked ICT process due to the complex emerged by Cr^{3+} ion and probe 5a. But, probe 5b showed seriously weak emissions centered at 490 nm due to the reflection of ESIPT and the isomeric effect of functional moieties. The addition of Cr^{3+} ions led to imparted intense emission because of switched "ON" CHEF effect and inhibited PET effect. Hence, Probe 5a and 5b show better sensitivity in the "ON-OFF" PET fashion. Probes 5a and 5b provide a 2:2 stoichiometry ratio as per the titration for Cr^{3+} (**Fig. 5**).

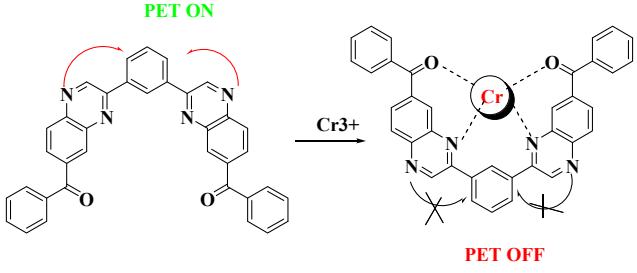

Fig. 6. Structure of fluorescence probe6 and binding with metal

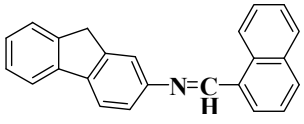

Fig. 7. Chemical structure of probe 7

To achieve low-level detection for Cr^{3+}, Probe 6 was developed out of a new Schiff base fluorescent moiety by Dinesh Kumar *et al* [41]. The stock solution was prepared by dissolving probe 6 in DMF: H_2O (4:1, v/v) and observed quenched fluorescence on the addition of Cr^{3+} ions into Probe 6. The quenching effect is attributed due to the metal ion having made a bond with the active center of the sensor and the PET process inhibited. The detection limit by Probe 6 was 0.5 μM. To stress the selectivity of probe 6 to Cr^{3+} vitro studies on empty HepG2 cells and Probe 6+ Cr^{3+} ions cultivated HepG2 cells were carried out then, resulting fluorescence was switched off in the presence of Cr^{3+} ions. This ensured the role of probe 6 for chromium ions in living cells (**Fig. 6**). A new type of fluorescent probe 7, designed by Hu et al. in which a naphthalene derivative ring was incorporated with a fluorophore, and both were connected through-C= N bond[42]. The synthetic probe 7 was found to detect Cr^{3+}ions in CH_3CN-H_2O (v/v, 7:3) exhibited a weak emission at 305nm without Cr^{3+} ions and displayed an intense fluorescence (923 times) on the addition of Cr^{3+} ions. Fluorescence enhancement of probe 7 reasoned as the formation of a complex with Cr^{3+}ions followed by oxidation by unstable C–N–O three-membered ring structure then, the structure build-up as an amide group (P-6-O), finally arrested cis-trans isomerization of imine group. The low detection limit by probe 7 was 63.1 nM (**Fig. 7**). Mukherjeeet *et al*., are interested in designing a probe 8 using a pyrene-based luminescent compound for the detection of Cr^{3+} ions[43]. Probe 8 without the addition of ions shows a weak fluorescence with a quantum yield of (Φ) 0.035. Upon the addition of Cr^{3+} ions, fluorescence enhancement was observed. The enhancement in fluorescence is due to Chelation–enhanced fluorescence by pyrine (4.3 times increment) in DMSO. For the first time, Derivative synchronous fluorescence spectroscopy (DSFS) study was performed to figure out the relation between probe 8 and Cr^{3+}. The LOD was calculated as 4.925×10^{-9} M with the limit of quantification is 1.64×10^{-8} M and the stoichiometry relation was found to be 2:1 (**Fig. 8**).

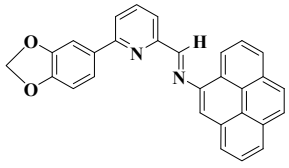

Fig. 8. Chemical structure of probe 8

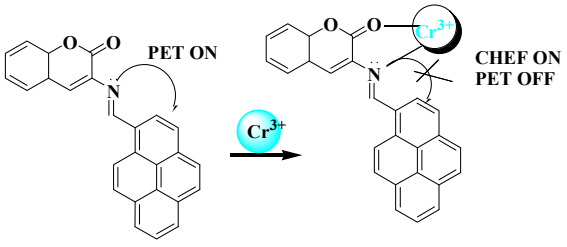

Fig. 9. Structure of fluorescence probe 9 and binding mechanism.

Two simple molecules have been associated to produce a novel probe 9; it was reported as an effective sensor for Cr^{3+} ions and some other trivalent cations[44]. A weak emission has been observed by probe 9 alone. After the addition of Cr^{3+} ions into probe 9 in an aqueous medium, outstanding fluorescence enhancement was achieved and obtained with color change during the assessment. The complex formation within probe 9 by the support of the Cr^{3+} ion produced inhibition of the PET effect and provoked CHEF. The stoichiometry ratio has been obtained as 1:1 between probe 9 and Cr^{3+} ions. It showed an exceptionally low detection range of 1.15 μM. On the biological survey, it displayed low cytotoxicity, and probe 9 allowed the detection of the range of Cr^{3+} in HDF cells (**Fig. 9**).

2.2 Fluorescence Probes for Ferric Ion (Fe^{3+})

Iron (III) is one of the considerable heavy metal ions which belong to group 8 in d-block elements. It can be significantly involved in the synthesis of organometallic compounds such as ferrocenium and it is an important cation in proteins like metalloproteins, ferredoxin, and cytochromes for various living organisms. Iron in ferrous form is the basic element for cell growth via carrying the oxygenated blood to the body cells with the aid of the hemoglobin unit of human blood and it helps the secretions of various enzymes that our body demand for functions of vital organs. Many biological molecules associated with Iron (III) are crucial for the functions of all organs. A diet with a low amount of iron will never help to prevent anemia. Instead, it will increase the severity of such disease. Both environmental damage and human health impairment can occur due to excess iron. According to the world health organization, the recommended level of iron (III) is 0.3mg/L [45-50].

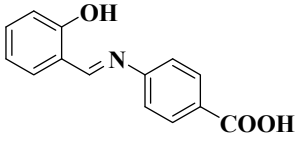

Fig. 10. Chemical structure of fluorescence probe 10

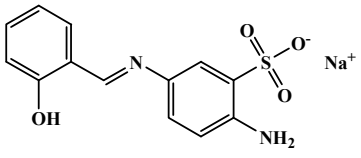

Fig. 11. Structure of fluorescence probe 11

A modest Schiff base probe 10 was synthesized by Singh *et al*., using the amino benzoic acid and salicylaldehyde. Probe 10 has been further reported for the detection of abundant iron metal (Fe^{3+}) in various solvent mediums[45]. Probe 10 was found to be an excellent sensor to detect Fe^{3+} because the addition of Fe^{3+} ion into probe 10 has brought quenching in the fluorescence intensity (Decreased more than 10-fold). Fluorescence quenching mechanism was based on the truth that on complex formation between probe 10- Fe^{3+} that promised lone pair of electrons of nitrogen atom has moved to empty d-orbital of Fe^{3+} because of the ICT process (**Fig. 10**). The probe 10-Fe^{3+}complex was found to be highly stable from its stability constant value. (Ka = 5.85 × 10^3 M^{-1}). New and highly selective Schiff base molecule 11 has been developed and used as a unique detector for Fe^{3+} ions in $H_2O$by *Çelik et al* [46]. Probe 11 expressed a deep fluorescence emission in an aqueous medium due to aggregation-induced emission (AIE), which has turned off after adding Fe^{3+} into it, and the color of the solution turned light yellow from light blue in front of a UV-visible lamp. Further, the complex of probe 11 and Fe^{3+} showed worthy absorption in the range of 295nm owed to the selectivity of probe 11 towards ferric ions in a water medium. The obtained detection limit was 1.29 μM for Fe^{3+} (**Fig. 11**). Another coumarin-linked acyl hydrazone Schiff base-based fluorescence probe 12 with outstanding sensing capability to Fe^{3+} ions in ethanol-water solution reported by Yang *et al* [47]. A fluorescence spectral study revealed that a strong fluorescence emission occurred at 378 nm due to isomerization in C=N,-NH group of probe 12, which was further quenched by adding an equivalent amount of Fe^{3+}contains solution into probe 12. This quenching is due to reversed isomerization of the probe. The low detection limit was 5.92 ×10^{-7} M for Fe^{3+} ion (**Fig. 12**).

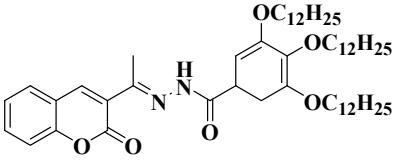

Fig. 12. Structure of fluorescence probe 12

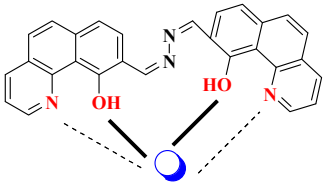

Fig. 13. Structure of fluorescence probe 13 and binds the Fe^3

Swaminathan *et al*. developed a fluorescent probe 13 and demonstrated its detection behavior for Fe^{3+} ions in real samples and biological media[48]. Probe 13 in MeCN showed feeble fluorescence emission owing to free-electron transfer between the binding unit and fluorophore. Relatively high-intensity emission of about a 382-fold increase was recorded as the addition of Fe^{3+} ions into probe 13. The quantum yield for complex formation is distinguished as Φ=0.32. Further, the interaction of water to the complex of Probe 13+ Fe^{3+} was tested and found quenching on the considerable amount of water. As a result, the intensity ratio of complex formation was 0.9985. The binding constant for [Probe 13+ Fe^{3+}] calculated 8.78×10^3 M^{-1}. The calculated LOD of probe 13 towards Fe^{3+} ion was 3.3 nM. Subsequently, probe 13 effectively recognized the presence of Fe^{3+} in the human serum sample (**Fig. 13**). A novel AIE passive colorimetric and fluorescent probe 14 was synthesized for the detection of Fe^{3+} ion and reported by Yin *et al*.[49] A solid fluorescence emission centered at 446 nm for free probe 14 on account of a rotation of intramolecular hydrogen bond in DMSO/H_2O (1:9, v/v, pH=7.2) in a solvent medium. Fluorescence quenching was observed for the complex [probe 14 + Fe^{3+}] at 472 nm after adding Fe^{3+} ions. This is due to the stumbling of the AIE process. Found no interruption by various other transition metals to probe 14as correlated by Fe^{3+} ions. Based on the fluorescence titration analysis, the relation between probe 14 and the Fe^{3+} ion was understood by two new isosbestic points one at 385 nm and another at 391 nm. The LOD of probe 14 was found to be 4.88×10^{-7} M with Fe^{3+} ions (**Fig. 14**).

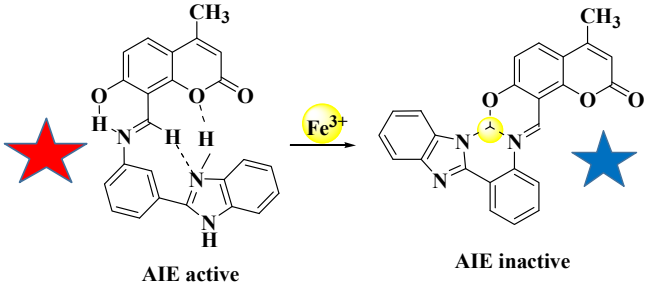

Fig.14. Structure of fluorescence probe 14 and binds the metal.

The benzothiazole moiety is popularly known for its two free electron-donating groups such as nitrogen and sulfur and can make a complex with a strong affinity to Fe^{3+} ions. Gong *et al*. reported probes 15a, and 15b for Fe^{3+} ions in water samples[50]. The probes 15a and 15b exhibited very good fluorescence performance peaks at 411nm and 421nm correspondingly. The association of those sensors with Fe^{3+}ion issued quenching immediately. In terms of binding ability by the probes hooks the metal ion with equal strength, exhibited binding constants are 3659 M^{-1} and 4156 M^{-1} respectively. Despite more than two binding sites, availability in two probes shows a 1:1 stoichiometry relationship. The detection limit

was 8.43μM for probe 15a and 5.86 μM for 15b and probes displayed low cytotoxicity. Those results confirmed the service of those probes to detect the Fe^{3+}ions in HeLa Cells (**Fig. 15**).

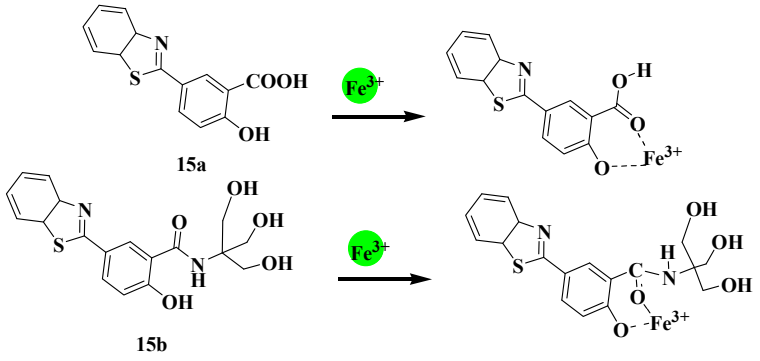

Fig. 15. Structure of fluorescence probe 15a, 15b, and binding mechanism

A hydroxyl naphthalene derivative was synthesized as a powerful probe16 for Fe^{3+} ion in DMSO-H_2O and reported by Ozdemir*et al* [51]. As per absorption analysis, probe 16 shows three different bands at 325, 378, and 474 nm in UV- Visible lamb. Upon the addition of Fe^{3+} ions into probe 16 and its shows, a blue shift and this is due to the formation of the complex with probe 16. Additionally, distinct-color fading was also noted in probe 16 by adding Fe^{3+} ions. These results account for the selectivity of the above probe16 to Fe^{3+} ions. The detection limit was found to be 3.473 μM for the probe 16-Fe^{3+}, which is relatively low according to the WHO standard (31.5 μM) (**Fig. 16**).

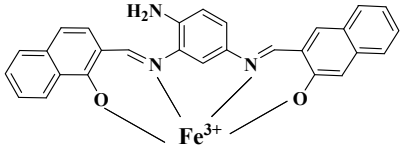

Fig. 16. Structure of fluorescence probe 16 with Fe^{3+}

2.3 Fluorescence Probes for Copper Ion (Cu^{2+})

Copper (Cu^{2+}) is graded as the world's third most available element on Earth. Any considerable deficiency of copper can also cause anemia, weakening of the nervous system, and diseases such as Parkinson's, and Alzheimer's in the human body. When the amount of copper exceeds its limit even if it's a very trace amount immediately, gives rise to the following weaknesses: neurological disorders, formation of ROS free radicals, Menkes and Wilson's diseases, and cost more trouble to the environment apart from collective applications. Hence, copper can be allowed in drinking water up to 1.3 mg which is very much mandated to avoid the gastrointestinal problem for humans according to WHO [52-54].

Liang *et al*. synthesized a hydrophilic naphthalimide-based Schiff base fluorescent probe 17 to detect Cu^{2+} ions in ethanol solution [55]. In fluorescence, the study found that probe 17 has given a strong emission at 532 nm while exciting at 436 nm. Upon the addition of Cu^{2+} ion into probe 17 ended a quenching in fluorescence due to the electron transfer raised from 1, 8-naphthalimide fluorophore to Cu^{2+} analyte. It was concluded that the effectiveness of probe 17 to bind the Cu^{2+} ion in phosphate buffer at pH 7.4. The fluorescence titration helped to calculate the detection limit as 0.37 nM for probe 17. The selectivity of probe 17 to Cu^{2+} ions was further examined in drinking water samples and achieved a great response (**Fig. 17**).

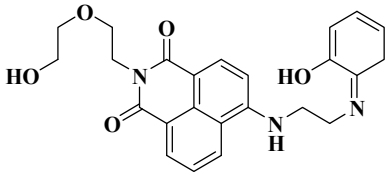

Fig. 17. Structure of fluorescence probe 17

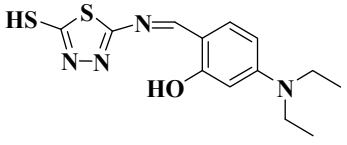

Fig. 18. Structure of fluorescence probe18

New Schiff-base-based probe 18 has been synthesized and characterized with minimum spectral analysis. The authors discussed its application to sensing Cu^{2+} ions in water samples by Ben *et al.*[56] The addition of Cu^{2+} ions, into probe 18 has given a fluorescence quenching and rapid color changes from yellow to brown on naked-eye observation along with showing no deviation by the addition of similar other metal ions, which help us to justify probe 18 selectivity towards Cu^{2+} ions. The detection limit of probe 18 to Cu^{2+} ions was 5.721×10^{-7}mol/ L and the stoichiometric ratio between probe 18-Cu^{2+} ions was 1: 1 (**Fig. 18**). A novel Schiff base-based fluorescence probe 19 has been designed by Wang *et al* and reported for the

detection of Cu^{2+} ions selectively and sensitively over other ions[57]. Further, the addition of Cu^{2+} ions into probe 19, displays deep fluorescence intensity at 472 nm in the emission spectrum with immediate color change. The visual change and fluorescence changes are due to the formation of a complex with probe 19- Cu^{2+} ions, which accounted for the selectivity of probe 19 for copper ions. The determined detection limit was 8.5×10^{-7} M in an aqueous medium (**Fig. 19**).

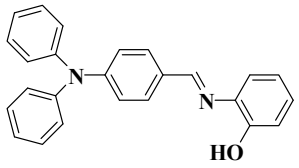

Fig. 19. Structure of fluorescence probe 19

The inclusion of the phenol group in Schiff base-based fluorophore probe 20 would respond to excellent detection of Cu^{2+} ions sensitively and it was reported by Manna *et al* [58]. On the screening for Cu^{2+} ions, probe 20 showed a strong yellow color under UV-Visible light and monitored an absorption peak at 394 nm for metal complexes as new points. It must be because of inhibited ICT process but during the interval addition of metals. The addition of the ions into probe 20 did not show any changes unless the addition of Cu^{2+} ions. A quenching effect of fluorescence was noted by the addition of Cu^{2+} ions which has taken justice for switching on ICT effect by concrete binding between probe 20 and Cu^{2+} ions and instant reduction free-electron richness by a couple of N and O atoms (**Fig. 20**).

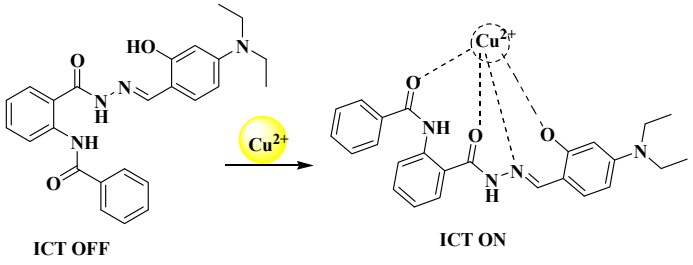

Fig. 20. Structure of fluorescence probe 20 and metal binding mechanism

A new organosulfur compound has been designed and reported for the sensible detection of Cu^{2+} ions by Sahu *et al*[59]. The polydentate ligand of probe 21 successfully detects Cu^{2+}ions with high quantum yields. The addition of Cu^{2+}ions into probe 21 in methanol-tris-HCl buffer (1:1 v/v, 5 mM, pH=7.2) brought corresponding redshift (322nm → 365nm) in the UV-Visible range with expected color change. The visual change and optical changes of probe 21 are due to the ICT effect upon binding with Cu^{2+}ions. The detection limit of probe 21 is estimated at 1.7μM for Cu^{2+} ions. The partnership between host-guest binding is noted as 2:1 (**Fig. 21**).

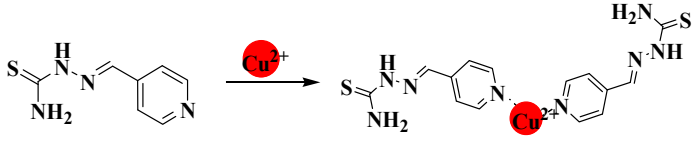

Fig. 21. Structure of fluorescence probe 21 and metal binding mechanism

Naphthalene derivatives are very good fluorophores and display a signal through different colors while the binding group reaches it. Naphthalene-based fluorescent and colorimetric probe 22 was reported by Gurusamy*et al*[60]. Probe 22 was utilized to focus on the selective sensing of Cu^{2+} ions in an aqueous medium over other competing metal ions. The addition of Cu^{2+} ions into probe 22 originated a promised color change from yellow to dark brown with a strong absorption peak at 540 nm. Further, with the addition of metal ions, the Cu^{2+} ions show fluorescence quenching and interrupts the ICT effect. The detection limit and stoichiometry ratio of Cu^{2+} ions in probe 22 were found to be 2.09 μM and a 1:1 binding site (**Fig. 22**).

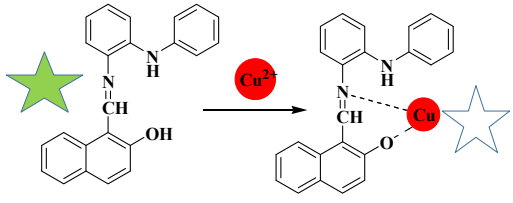

Fig. 22. Structure of fluorescence probe 22 and metal binding mechanism.

A magnificent fluorescent probe 23 was synthesized by S. Anbu *et al*[61] and promoted probe 23 as a sensor for Cu^{2+}ions in CH_3CN/50 mM HEPES buffer at pH = 7.4. The recognition of Cu^{2+} ions was demonstrated through spectral studies. The emission peak of probe 23 at 515nm (excitation at 380 nm) decreased (9-fold) upon the addition of Cu^{2+}ions (2 equiv) and shows a redshift initially due to the photoinduced electron transfer (PET) mechanism. This change is related to the contribution of a phenolate O atom and two N atoms from azomethine and benzimidazole respectively followed by the arrested PET process. Based on the absorption titration data the stoichiometry for the metal complex has to be 1:2. The association constant of probe 23-Cu^{2+} ions were measured as 1.63×10^{10} M^{-2}. Cell viability test confirmed the support of probe 23 to investigate the Cu^{2+} ions in biological cells (**Fig. 23**).

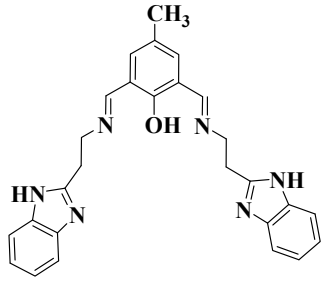

Fig. 23. Structure of fluorescence probe 23 and metal binding mechanism.

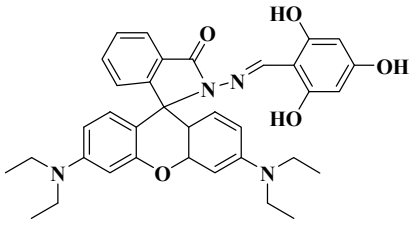

Fig. 24. Chemical structure of fluorescence probe 24

Cheah *et al.* designed a new rhodamine-based probe 24 for Cu^{2+} ion detection and proved that it is a unique class of sensor due to high sensitivity and low-level detection limit[62]. A pink color solution occurred upon the addition of Cu^{2+} ions into probe 24. These results confirm the suitability of probe 24 towards Cu^{2+} ions over other competing ions. The addition of Cu^{2+} to the solution of probe 24 displays an absorption peak at 559 nm, owing to the involvement of the spirolactam ring of probe 24 in metal binding. Showed fluorescence quenching at the end of the study on the addition of Cu^{2+} ions into probe 24. Have not found any suspicious interference with other metals. The detection limit was found to be 0.48 μM for Cu^{2+} ions. The cytotoxic nature of probe 24 with colorectal adenocarcinoma cells displayed low cytotoxicity with Cu^{2+} ions (**Fig. 24**). A new pyridine-based probe 25 was designed and synthesized by Mohanasundaram *et al* and reported for the trace detection of Cu^{2+} ions in CH_3CN/H_2O (7:3, v/v) medium[63]. The binding tendency of probe 25 towards Cu^{2+} ions reveals the visible color change from yellow to cyan. Subsequently, the addition of Cu^{2+} ions into probe 25 showed higher fluorescence intensity. These observations are due to the intervention on the isomerization by the imine group followed by the opened-up CHEF process while the strong affinity of probe 25 to Cu^{2+} ions. The detection level for Cu^{2+} was 0.25 μM. Probe 25 gives its contribution to Cu^{2+} ions in a 1:1 ratio (**Fig. 25**).

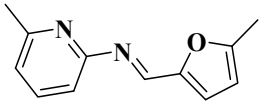

Fig. 25. Structure of fluorescence probe 25

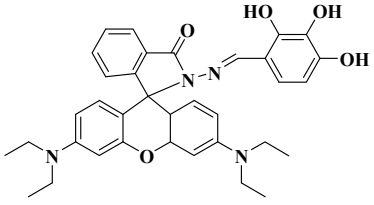

Fig. 26. Structure of probe 26

A sensor showing different sensitivity towards Cu^{2+} ions based on different solvents is another area of research. Probe 26 was synthesized based on rhodamine-based Schiff base probe 26 by Chan *et al* and reported for the detection of Cu^{2+} ions in the different solvent mediums[64]. Probe 26 was shown a band at 558nm and colorless probe 26 has turned into pink upon the addition of Cu^{2+} ions. It might be the opening of the spirolactam ring in rhodamine molecules in almost all the solvents such as ethanol, methanol, acetonitrile, DMSO, and DMF. The estimated detection limit for probe 26-Cu^{2+} is 1.40 x 10^{-7} M. The reversibility character of probe 26+Cu^{2+} ions was investigated by the EDTA titration method resulting in a strong overlap between probe **26** and Cu^{2+}. These results concluded that probe 26 forms a strong coordination compound with acceptor moiety. The interaction between host-guest species was found to be a 1:1 ratio (Fig.26). Dehydroacetic acid coupled with Schiff base-based probe 27 and employed in the detection of Cu^{2+}ion by Vashisht *et al*[65]. Probe 27 demonstrates a color change from yellow to bluish-green on the instant addition of Cu^{2+} ions. Two absorption peaks were found for free probe 27 in the UV-Visible region due to switching the "ON" Intramolecular charge transfer (ICT) effect between the -NH group and the benzyl ring. After the addition of Cu^{2+} ions into probe 27 showed a blue shift and switched "OFF" the ICT mechanism. This study probes 27 detects the Cu^{2+}ions in organic-aqueous samples. The association constant was observed as 5.928×10^4 M^{-1}. The selectivity of probe 27 towards other cations such as Ag^+, Al^{3+}, Ba^{2+}, Ca^{2+}, Cd^{2+}, Ce^{3+}, Co^{2+}, Cr^{2+}, Fe^{2+}, K^+, Mg^{2+}, Na^+, Ni^{2+}, Pb^{2+}, Zn^{2+}, Hg^{2+}, Mn^{2+} and Fe^{3+} was tested and observed no response with probe 27-Cu^{2+} (**Fig. 27**).

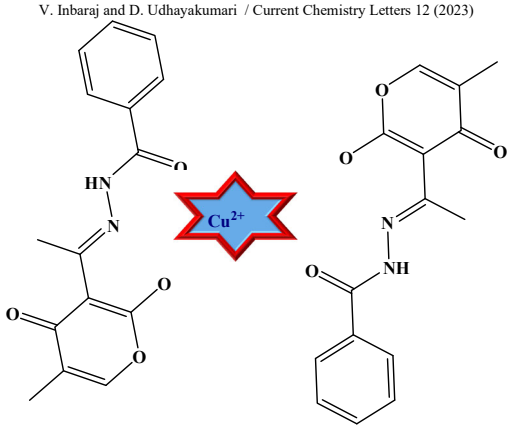

Fig. 27. Structure of probe 27

2.4 Fluorescence Probes for Zinc Ion (Zn^{2+})

Zinc is the second most abundant transition element in earth's crusts; it's a vital metal that acts as essential nutrition to humans while taken through various means and aids in insulin generation in the human body. Zinc minerals also play an important role in some biological reactions in our body like metabolism, cell growth, cell division, good immune system, and reproduction process. A decrease in the concentration of Zn^{2+}ions can cause a reduction in cell growth and loss of secreted insulin. The excess level of Zinc could bring cognitive diseases like Alzheimer's, Parkinson's, Menkes diseases, and lateral sclerosis. Apart from the biological applications, play as an essential source for important industrial operations. So the recommended dietary allowance level of zinc in the human body is 8mg per day as the United revealed in a case studies[66-75].

A turn-on fluorescence probe 28 based on a new Schiff base was developed and its selectivity to Zn^{2+} in the middle of competitive metal ions was demonstrated with nil interference by the contribution of Kumar *et al*[67]. The gradual addition of Zn^{2+} into probe 28 in the DMF solution instantly raised a strong fluorescence signal at 509nm with a 54-fold increment. The fluorescence quantum yield had calculated as $\Phi_F = 0.0207$. It was noticed that as complex formation (probe 28+Zn^{2+}) the C=N unit of probe 28 could strongly bind with metal ions with a binding constant was $K_a = 7.8x10^4\ M^{-1}$. The limit of detection by probe 28 to Zn^{2+} was 8.6 x 10^{-9} M (**Fig. 28**).

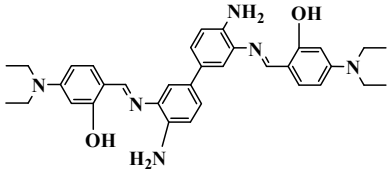

Fig. 28. Structure of fluorescence probe 28

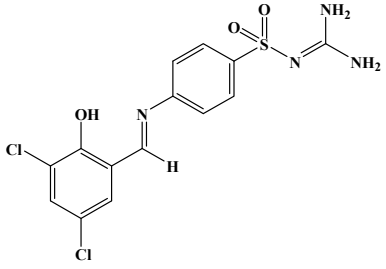

Fig. 29. Structure of fluorescence probe 29

Schiff base-based Sulfonamides derivatives were developed by Mondal *et al.* and reported to recognize the trace level of Zn^{2+} ions in an aqueous medium [68]. With the countable addition of Zn^{2+} ions to probe 29 stock solution, a prompt greenish-yellow bright color appeared and there was a strong emission at 514 nm (λ_{ex}= 405 nm). The fluorescence intensity is due to the ESIPT effect and has been quenched by the presence of Zn^{2+} means that the ESIPT effect has been overcome by complex formation. The quantum yield and the stoichiometry ratio for Zn^{2+} and probe 29 were calculated to be Φ=0.53 and 1:2 respectively. According to the Benesi-Hildebrand formula, the binding constant and detection limit was calculated to be $K_d = 1.35\times10^4\ M^{-2}$ and 37.4 nM for Zn^{2+} ions (**Fig. 29**).

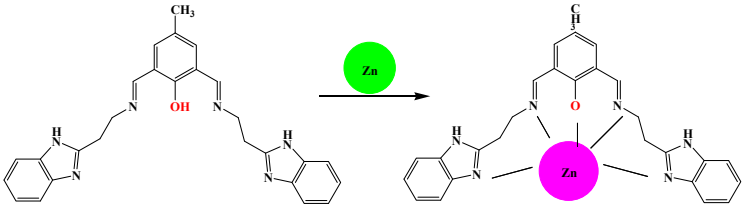

Fig. 30. Structure of fluorescence probe 30 and its binding mechanism

Anazomethine coupled benzimidazole derivative-based probe 30 has been developed for the detection of Zn^{2+} ions in CH_3CN/50 mM HEPES buffer at pH = 7.4[61]. A bright fluorescence enhancement (4-fold) has been observed on the incremental addition of Zn^{2+}ions into probe 30. The enhanced fluorescence may be because the metal ion can interact with the binding sites of the receptor in its excited state. The binding constants and the binding ratio of probe 30 for Zn^{2+} ions were calculated to be 2.0×10^4 M^{-1} and 1:1 respectively. The nanomolar detection limit was calculated and the sensing ability was further extended to living cells to explore the Zn^{2+} ions (**Fig. 30**). Rout *et al*. designed a brand-new imine -quinidine-based probe 31 and reported the detection of Zn^{2+} ions in an aqueous medium[69]. Probe 31 was characterized through simple spectroscopic studies. The inclusion of Zn^{2+} into probe 31 headed towards fluorescence enhancement with an almost 26-fold increase. The inclusion of Zn^{2+} ions blocked the PET process of probe 31 and the fluorescence effect is turned on in the presence of Zn^{2+} ions. Based on the fluorescence titration, the detection limit has been calculated as 2.04×10^{-6}M for Zn^{2+}. The ESI-MS data of complex [probe 31+Zn^{2+}] reveals that the complex depends on a 1:1 ratio (Fig. 31).

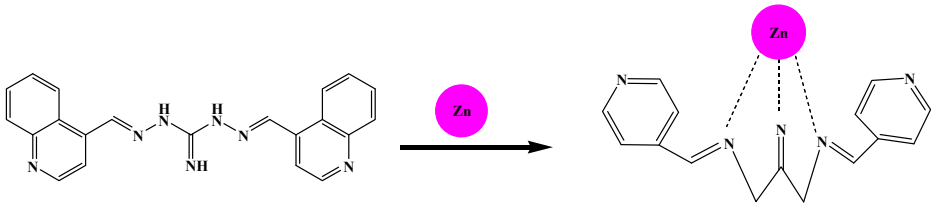

Fig. 31. Structure of fluorescence probe 31 and binding mechanism

Sun *et al*. designed and reported a fluorescence "OFF-ON" based coumarin derivative for the quantitative analysis of Zn^{2+} ions[70]. Probe 32 alone has a tedious fluorescence response due to free electron transfer. The addition of Zn^{2+} to probe 32 resulted in a default redshift (8-fold increment) with an enhanced fluorescence spectrum. The 1:1 stoichiometry ratio was found between probe 32 and Zn^{2+} ions. The free electrons of N atoms and O atoms are engaged and form the network between probe 32 and the Zn^{2+} ions. Hence, the PET effect was put off and CHEF was launched. The detection limit of probe 32 with Zn^{2+} ions was calculated to be 3.26×10^{-7}mol/L (**Fig. 32**).

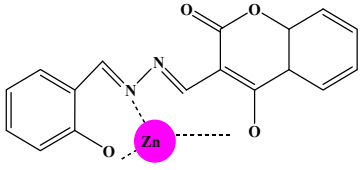

Fig. 32. Structure of fluorescence probe 32

Coumarin and aminopyrazine acylhydrazone coupled fluorescence probe 33 has been developed by Xue *et al*. and reported for the detection of Zn^{2+} ions in an aqueous medium[71]. A red-shifted fluorescence emission spectrum was observed upon the addition of Zn^{2+}ions into probe 33. In an aqueous medium (99.5 %) the emission band shifted to the blue region from 555nm to 524 nm (solvent effect). The fluorescence intensity ratio of probe 33 with Zn^{2+} ions is F_{628}/F_{555}. The enhanced fluorescence is due to the coordination of Zn^{2+} ions with the lone pair of electrons in probe 33 which created a metal complex in a 1:1 ratio. Except for Cu^{2+} ions, other metal ions didn't show any fluorescence changes when interacting with probe 33. Upon the addition of Cu^{2+} ions, slight incline fluorescence was observed. The detection limit and association constant of probe 33-Zn^{2+} were found to be 3.52µM and 5.59 x$10^3$$M^{-1}$ respectively. Probe 33 responded well towards Zn^{2+} ions detection in an aqueous medium and was effectively used to find stained Zn^{2+} ions in biological cells (**Fig. 33**).

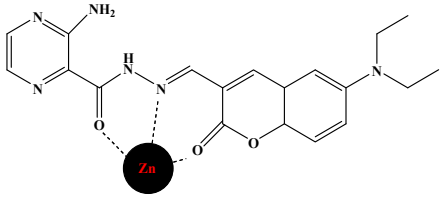

Fig. 33. Structure of fluorescence probe 33 for Zn^{2+}.

Organic probe 34 has been fabricated by connecting piperidine and salicylaldehyde derivatives and reported for the selective detection of Zn^{2+} ions in an aqueous solution[72]. Upon the addition of various interference ions into probe 34, Zn^{2+} ions only demonstrate a significant increase in fluorescent intensity band in an aqueous medium. The fluorescence enhancement is due to the interaction of Zn^{2+} ions to the donor center of probe 34. Further, the incremental addition of Zn^{2+}

ions exhibit a linear relationship in the emission line. The detection limit for probe 34-Zn^{2+} was calculated to be 5.34×10^{-8} M (**Fig. 34**).

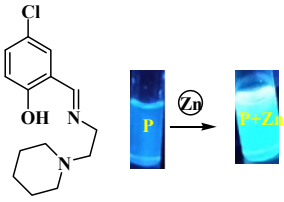

Fig34. Structure of probe 34

Maity *et al*. have reported an effective fluorescence probe 35, to sense Zn^{2+} in water, methanol (9: 1, v/v) medium[73]. They focused more on overcoming the high expenditure for the preparation of a chemosensor and applying it to detect the Zn^{2+} ion on the spot. In the presence of Zn^{2+} ion after gradually being added into probe 35 have noticed a constant enhancement in fluorescence signal intensity but at one equivalent of Zn^{2+} ion to probe 35 has shown the strongest fluorescence emission signal with 32 fold high. Based on the above effect, we have confirmed the suitability of probe 35 to Zn^{2+} ion. The mechanism was the formation of a complex molecule between probe 35-Zn^{2+} ions via inhibition of the PET process. So probe 35 has become the effective chemosensor for Zn^{2+} ions with high sensitivity and the superior detection limit is 4.41×10^{-7} M (**Fig. 35**).

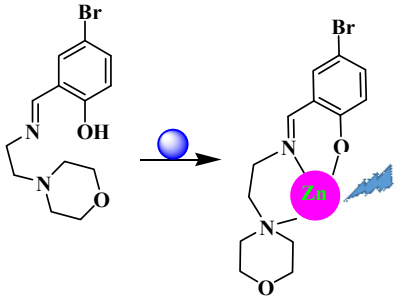

Fig. 35. Structure of probe 35

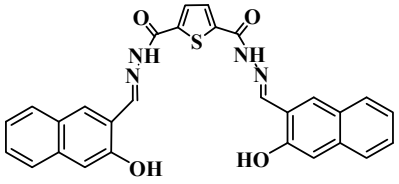

Fig. 36. Structure of probe 36

Another, Schiff base-based fluorescent molecule, which could be optically sound in nature, probe 36 was synthesized by Mathew *et al*[74]. Its sensing property towards Zn^{2+} has been revealed through Turn-On fluorescence performance on the incremental addition of Zn^{2+} into probe 36. Further, it was confirmed via a highly notable color change in the presence of Zn^{2+} (color of the probe 36 has turned yellow from light yellow). The fluorescence "OFF" and "ON" mode of probe 36 with Zn^{2+} and without it, is reasoned as the chelation-enhanced fluorescent effect (CHEF) and the photo-induced electron transfer (PET). The detection limit of probe 36 to Zn^{2+} ion was 1.51×10^{-7} M, based on the fluorescence titration procedure. The measured value found is a much lower value than the allowed value of Zn^{2+} ions in domestic water as per USEPA standard(70 μM) (**Fig. 36**). Bountiful, analogous fluorescent probes have been established over the era for Zn^{2+} ion in organic solvents along with dull fluorescence effect but probe 37 which was designed and reported by Park, *et al*. for Zn^{2+} ion, has held special attention owing to its selectivity and sensitivity in UV-visible light and able to sense the Zn^{2+} ion is a fully aqueous medium[75]. The sudden increase in fluorescence emission on the addition of Zn^{2+} ions into probe 37 has helped to recognize the sensing ability of probe 37 for cation. ^{1}H NMR analytical data helped to trace the binding mechanism of probe 37 that the O atom of the phenyl group and lone pair of electrons from the imine N group of probe 37 contributed to the compound formation with Zn^{2+}. The detection limit of probe 37 towards the Zn^{2+} ion was calculated to be 1.07 μM (**Fig. 37**).

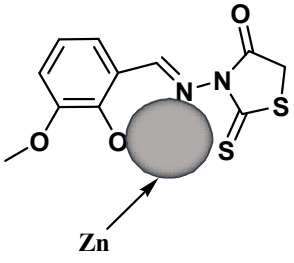

Fig. 37. Structure of probe 37

2.5 Fluorescence Probes for Cadmium Ion (Cd^{2+})

Cadmium (Cd^{2+}) plays a crucial role in various industries like alloys, coloring agents, Ni-Cd batteries, phosphate fertilizers, and the electroplating of metal. Cadmium (Cd^{2+}) ions can be part of the air, water, and plants at different levels. It causes severe environmental and health problems, including lung, prostatic, and renal cancers. Standard care should be taken to constantly measure Cd^{2+} in various samples. This is an hour of need to control beyond the allowed limit. According to the WHO, the recommended level of cadmium in drinking water is 3.0 μg l^{-1}. Therefore, it has been a great challenge to develop a Cd^{2+}-selective fluorescence sensor with a low level of detection[76-79].

A novel Schiff-base-based compound has been synthesized as a fluorescence probe 38 and evaluated its sensing competence for Cd^{2+} ion in ethanol medium[80]. The addition of Cd^{2+} ions into probe 38 exhibited a strong fluorescence signal, which was unique to the intervention of Cd^{2+}. (Intensity was 490 nm). Probe 38 had a high feasibility for the C=N isomerization effect, which had been reserved while the Cd^{2+} ion was added into the probe which has become a method of sensing the metal ion. The calculated detection limit of probe 38 to Cd^{2+} was 1.1×10^{-6} M. Probe 38 showed a one-to-one correlation with Cd^{2+} ions (**Fig. 38**).

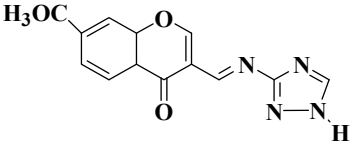

Fig. 38. Structure of probe 38

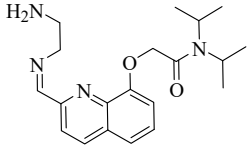

Fig. 39. Structure of probe 39

Quinoline-based Schiff base fluorescence probe 39 has been synthesized and characterized using different spectroscopic techniques. The sensing ability of probe 39 was tested and reported for the selective detection of Cd^{2+} ions in acidified methanol-water solution (10%-95%,v/v)[81]. An absolute red shift band at 246 nm was noted on the addition of Cd^{2+} into probe 39. It indicated that when Cd^{2+} approaches probe 39, the condition turns to the compound formation and promotes the fluorescence intensity. The detection limit of probe 39 toward Cd^{2+} was calculated to be 2.4×10^{-9} M. The sensitivity and selectivity of probe 39 for Cd^{2+}ions have been optimized in front of Hg^{2+} ions and other cations, which have given nil deviation at fluorescence examination (**Fig. 39**). An amide to the imidic acid tautomeric product was synthesized and its binding competency towards the Cd^{2+} ion was stated by *Liu et al*[82]. The addition of Cd^{2+} into the fluorescent probe 40 conveyed a blue shift along with an intense fluorescence emission band at 567 nm (65-fold, Φ = 0.32) in HEPES buffer at pH 7.4 (0.5% DMSO). Even though some of the ions like Pb^{2+}, $Hg^{2+,}$ and Zn^{2+} were also given a fluorescence enhancement while adding them into probe 40 but the intensity of the signals was not up to the level to compare the fluorescence enhancement that happened by the addition of Cd^{2+}. Therefore, the selectivity of probe 40 to Cd^{2+} has no competition with any other metal ions. As per ^{1}HNMR data, the amide NH group in probe 40 has shifted as an imidic acid functional group, which would be that the Cd^{2+} ion had been caught by probe 40. The binding stoichiometry ratio was calculated as 1:1 between probe 40 and Cd^{2+} ions by job plots (**Fig 40**).

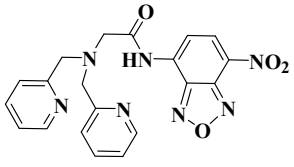

Fig. 40. Structure of probe 40

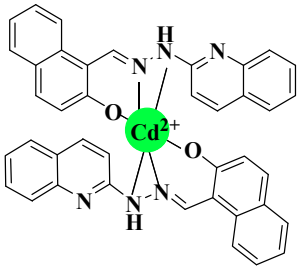

Fig. 41. Structure of probe 41

D. Mohanasundaram *et al* and co-workers elucidated a probe 41 and reported for the selective sensing of Cd^{2+} ions[83]. In the presence of a visible light probe 41 has turned into yellow-orange from colorless and showed strong fluorescence intensity (37-fold) on the inclusion of Cd^{2+} ions. There was a restriction on the C=N group followed by switching on CHEF of fluorophore while adding Cd^{2+} ions with high quantum yield (Φ = 0.326). The stoichiometry relation for the complex was 2:1 with an association constant for Cd^{2+} 1.77×10^{5} M^{-1}. The measured LOD to Cd^{2+} was 1.48×10^{-8}M which is less than the allowed amount (**Fig. 41**). A novel chemosensor 42 based on Schiff base has been developed for cadmium (Cd^{2+}) ions[84]. Probe 42 has been employed to select the Cd^{2+} ion in the prepared solution (DMF-H_2O) and the sensing character of probe 42 to Cd^{2+} was confirmed via fluorescence examination. A fluorescence enhancement has been noticed with a 9-fold increase when Cd^{2+} was added into probe 42, owing to the combined ICT (intramolecular charge transfer) and chelation-

enhanced fluorescence (CHEF). Further, the color of raw probe 42 (light yellow) transformed into reddish-orange on the coordination of probe 42 with the Cd^{2+} ion. The association constants and stoichiometry of probe 42-Cd^{2+} ions were calculated to be 1.17×10^4 M^{-1} and 1:1 respectively (**Fig. 42**).

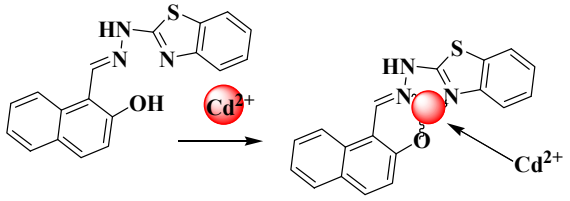

Fig. 42. Structure of probe 42

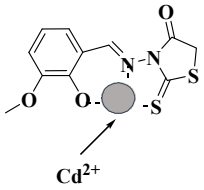

Fig. 43. Structure of probe 43

A synthetic molecule probe 43 has been developed via linking 3-amino-2-thioxothiazolidin-4-one and 2-hydroxy-3-methoxylbenzaldehyde moieties by Park *et.al* for Cd^{2+} ion in an aqueous environment[75]. The successful addition of Cd $^{2+}$ (3.5 equivalent) to probe 43 in an aqueous medium has yielded a rational fluorescence emission with a detection limit of 1.37 μM. ^{1}H NMR data reveal that the phenolic oxygen of probe 43 might be one of the binding sites for Cd^{2+}ion. Further, it has been confirmed through FT-IR analysis that imine and thiocarbonyl groups of probe 43 were also binding sites. The effectiveness of probe 43 to cadmium ions has been verified in real samples (**Fig. 43**). Chen *et al*. and group reported a fluorescence probe 44 for the profound detection of Cd^{2+} ions in the water-alcohol system[85]. The gradual addition of cadmium ions into probe 44 has inhibited the photoinduced electron transfer (PET) effect and launched the chelation-enhanced fluorescence (CHEF) effect of the chemosensor as the probe is more combined with Cd^{2+}. On fluorescence scrutinization, adding Cd^{2+} into probe 44 rewarded an intense fluorescence emission at 530 nm along with the distinct color change from no color to yellow in colorimetric analysis attributed the role of probe 44 to trace Cd^{2+} quantitatively. Probe 44 detects Cd^{2+} at a very low level (LOD = 41.0 nM)) and binds in the range of 1:1 stoichiometry. The detection behavior and practical applicability of probe 44 to Cd^{2+} were further studied by using a test strip kit. The test strip turned yellow instantly after it plunged into [probe 44 - Cd^{2+}] solution (**Fig. 44**).

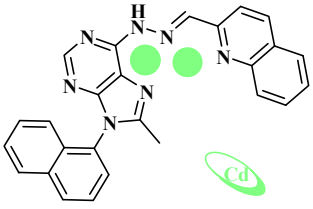

Fig. 44. Structure of probe 44

2.6 Fluorescence Probes for Cobalt Ion (Co^{2+})

Cobalt (Co^{2+}) is a naturally occurring element that does have beneficial applications and plays an important role in the metabolism of iron and the synthesis of hemoglobin, it is also the main component of Vitamin B_{12} and other biological compounds. Cobalt has been added to pigments to produce a distinct blue color. Lithium-ion batteries contain cobalt. In the medical field, cobalt-60 is used in radiotherapy and for sterilizing medical equipment. Cobalt is used to treat anemia in pregnant women because it stimulates the production of red blood cells. Cobalt deficiency in the human body may lead to pathological conditions and it is also a significant environmental pollutant. However, too high concentrations of cobalt may damage human health. When we breathe in too high concentrations of cobalt through the air we experience lung effects, such as asthma and pneumonia. Elevated concentrations of cobalt uptake result in health problems like vision problems, heart problems, thyroid damage, vomiting, and nausea.

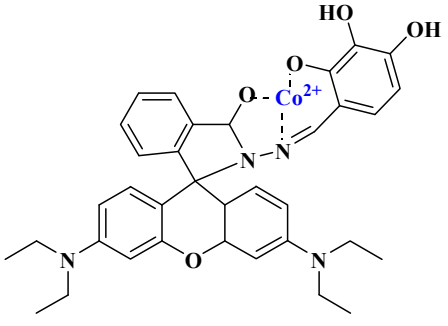

Fig. 45. Structure of probe 45

Rhodamine-bonded Schiff base probe 45 was designed and reported for Co^{2+} in MeCN/HEPES buffer (7:3, v/v, pH 7.0) and DMF/HEPES buffer (7:3, v/v, pH 7.0[64]. The addition of Co^{2+} into probe 45 displayed a brand-new absorption band of 558 nm from nil absorption of the free probe and a significant color change from colorless to pink was obtained. The close contact of Co^{2+} with the binding sites of probe 45 may be the reason for the strong absorption at 558 nm. The detection limit of probe 45 for Co^{2+} was 4.42 x 10^{-8} M. Probe 45 shows an excellent association constant with Co^{2+} as 6.46×10^{3} M^{-1} (**Fig. 45**). The color of filter paper turned pink from colorless as it immersed in an aqueous solution of Co^{2+}. Based on the cell viability examination of probe 45 on CCD-18 Co and HT-29 cells, the very good biocompatibility of probe 45 has been justified. A detection of Co^{2+} ions based 1-hydrazinophthalazine hydrochloride and imidazole-2-carboxaldehyde coupled to probe 46 has been reported by Rha *et al*. and group[86]. Upon the addition of the Co^{2+} ion, probe 46 demonstrates three different peaks at 270 nm, 315 nm, and 450 nm, and color change has been monitored from colorless to yellow in visible light. The above supportive conversion has confirmed the applicability of probe 46 to Co^{2+}. The other competing ions Mn^{2+}, Ca^{2+}, Al^{3+}, K^{+}, Cu^{2+}, Pb^{2+}, Ni^{2+}, Zn^{2+}, Cr^{3+}, Ag^{+}, Cd^{2+}, Fe^{3+}, Mg^{2+}, Hg^{2+}, Ga^{3+}, Fe^{2+}, Na^{+}, and In^{3+} didn't show any changes in the optical spectrum with probe 46. Based on the Job plot data probe 46 shows a 2:1 stoichiometry ratio with $Co^{2+}$and there is a much lower detection limit by probe 46 towards Co^{2+} ions (65 nM). The complex interaction of the paramagnetic tendency of Co^{2+} ions was confirmed based on the NMR spectrum. Hence, probe 46 would be an effective tool to detect another heavy metal ion (**Fig. 46**).

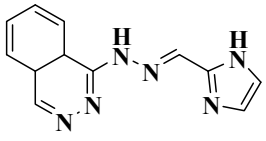

Fig. 46. Structure of probe 46

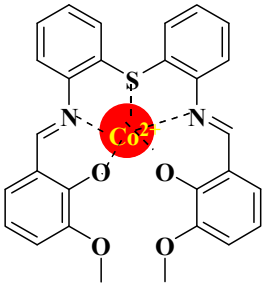

Fig. 47. Structure of probe 47

A new colorimetric Schiff base probe 47 has been developed and identified that probe 47 was a potential sensor for Co^{2+} Kim *et al*. in chemical media [87]. The addition of Co^{2+} to probe 47 reported a color change from colorless to yellow under the UV lamp. It was not observed while the other ions interacted with probe 47. The addition of Co^{2+} into probe 47 showed a tremendously increased absorption band at 420 nm with a 1:1 stoichiometry ratio. Probe 47 provides a significantly low detection range for Co^{2+} (0.66 µM) (**Fig. 47**). Pungut *et al*. and co-workers have reported a Schiff base-based chemosensor for Co^{2+} ions detection in an aqueous medium[88]. The color of probe 48 suddenly turned from colorless to yellow while adding Co^{2+}. The visual color transformation was due to the origin of delocalized xanthene in the rhodamine group and the broken spirolactam ring of probe 48. The detection limit of probe 48 for Co^{2+} was found to be 4.8×10^{-1}µM. It's proven that probe 48 can encounter the Co^{2+} without the competition of other ions with a 1:1 stoichiometry ratio. About 85 % CCD-18Co cells and 59% of HT-29 cells have not been destroyed by probe 48 even after being incubated for 72 hrs attributed to the low cytotoxicity of the probe (**Fig. 48**).

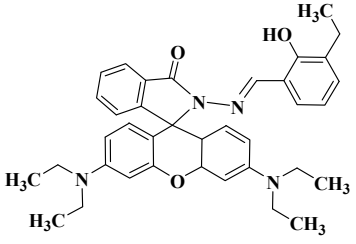

Fig. 48. Structure of probe 48

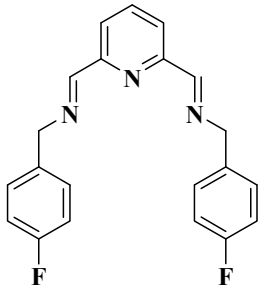

Fig. 49. Structure of probe 49

Alamgir *et al*. designed a candid Schiff base-based probe 49 and reported the detection of Co^{2+} in water-methanol[89]. The addition of Co^{2+} in probe 49 brought immediately a deep orange color from light blue and observed absorption peaks at 370 nm and 570 nm under UV-visible light due to binding sites being held in metal complex formation between probe 49 and Co^{2+}. The competitive colorimetric analysis observed with Cr^{2+}, Mn^{2+}, Fe^{3+}, and Zn^{2+} established no notable color change rather than the presence of Co^{2+}. The binding constant value of probe 49 + Co^{2+} system was log k = 4.5. This obtained value has been compared with other report values and found this is a higher value (log K = 4.4) in the HEPES buffer and a thiourea-based 1, 8-naphthalimide (log K = 4.1) in CH_3CN/HEPES (4/1, v/v) (**Fig. 49**).

2.7 Fluorescence probes for Mercury ion (Hg^{2+})

Mercury (Hg^{2+}) is well known as one of the most toxic metals and is widespread in air, water, and soil, generated by many sources such as gold production, coal plants, thermometers, barometers, caustic soda, and mercury lamps. As it can cause strong damage to the central nervous system, the accumulation of mercury in the human body can lead to various cognitive and motor disorders, and Minamata disease. A major absorption source is related to daily diet such as fish[90-91].

Probe 50 has been synthesized via a simple method and found to be suitable for the sensible detection of Hg^{2+} selectivity in an aqueous organic medium[69]. Under UV-Visible light, an elite color change happened from yellow to red with the addition of Hg^{2+}. Additionally, a notable absorption band at 440 nm was recorded. It concluded that probe 50 could detect the Hg^{2+} ion in methanol-tris buffer (1:1). Recognition of Hg^{2+} by the support of probe50 attributed to the following changes that unfolding of LMCT effect and energy gap lowered in the ICT process. As per the report obtained by the Mass spectroscopy study, the stoichiometry probability was found to be 1:2 ratios (**Fig. 50**).

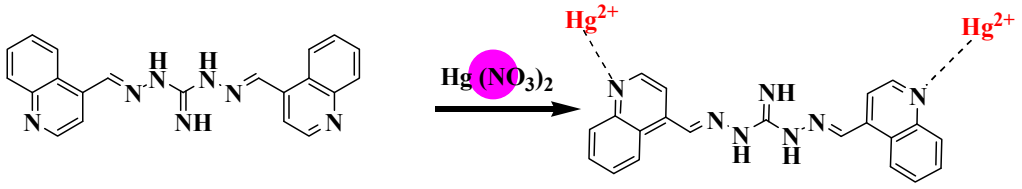

Fig. 50. Structure of probe 50

Musikavanhu *et al*. reported a chromophore 51[92] for sensing Hg^{2+} in HEPES buffer media. The bare probe 51 has shown intense fluorescence emission at 480 nm. The incremental addition of Hg^{2+} ions into probe 51 has quenched the fluorescence significantly. This suppression in the fluorescence of probe 51 is due to the addition of Hg^{2+} due to the CHEQ effect. Based on the Job plot the probe 51+ Hg^{2+} ions were found in a 2:1 ratio and the detection limit of probe 51 was found to be 23.4 nM. Interestingly it has been observed that it's unique where both dynamic and static fluorescence quenching occurs together. Based on the stern-Volmer equation ($F°/F=1+k[Q]$) the binding constant was calculated to be 5.54×10^6 L mol^{-1} (**Fig. 51**).

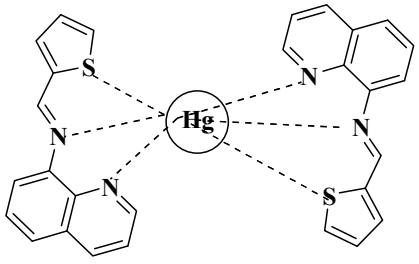

Fig. 51. Structure of probe 51

A precise fluorophore probe 52 was developed by Huang *et al.* to detect Hg^{2+} ions in THF/H_2O [93]. Peak shifting has been noted from centered at 395 nm to 459 nm, after adding Hg^{2+} into probe 52 under UV-visible spectra. Fluorescence competitive experiments was conducted with Ag^+, Ba^{2+}, Cu^{2+}, Co^{2+}, Cd^{2+}, Fe^{3+}, Fe^{2+}, K^+, Na^+ Ni^{2+}, Pb^{2+}, Sr^{2+}, Zn^{2+} and Hg^{2+} in THF/H_2O, fluorescence emission obtained at 505nm in the addition of Hg^{2+} . There was no such deviation noted with other cations. A low detection limit of probe 52 to Hg^{2+} was 2.78μM. Under both sunlight and UV-visible light (365nm), a distinct color change has been observed in the test strip while it was immersed in Hg^{2+} containing probe 52. Confocal fluorescence images of Hg^{2+} in zebrafish support the biological application of Probe 52 and low toxicity (**Fig. 52**).

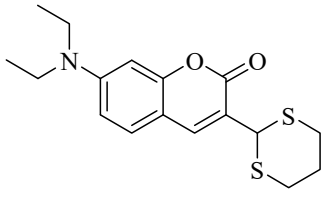

Fig. 52. Structure of probe 52

3. Conclusion

Even a trace amount of these d-block elements will cause deadly diseases in humans and impart environmental degradation. Designed organic molecules are required to trace them in the samples of environment, water, and biological species. Schiff base-based chemosensors have an excellent binding affinity towards metal ions. So Schiff base-based

fluorescent probes were employed to detect poisonous d-metals in low-level detection. Fluorescence studies between receptors and analysts are highly selective and sensitive, therefore, can utilize this technique to sense metal cations effortlessly. In this short *review,* various Schiff base-based fluorescence probes and their fluorescence sensing mechanism, and detection tolerance levels towards various d- metal ions have been discussed and this report was made based on current studies that focused on this area, in recent years. Most of the reported fluorescence probes detect d-metal ions successfully in different solvent media. This *review* will aid the readers to design a novel fluorescence probe for the effective detection of distinct d-metal ions in low-level detection**.**

Competing Interests

The authors declare that they have no competing interests.

Consent for publication

Not Applicable

Ethics approval and consent to participate

Not Applicable

Funding

No funding was received for this work.

Availability of data and materials

All data underlying the results are available as part of the article and no additional source data are required.

Author's Contributions

The author confirms the sole responsibility for the manuscript preparation.

References

[1] Asiri, A.M., Al-Ghamdi, N.S.M., Dzudzevic-Cancar, H., Kumar, P., Khan, S.A. (**2019**) Physicochemical and Photophysical investigation of newly synthesized carbazole containing pyrazoline-benzo thiazole as fluorescent chemosensor for the detection of Cu^{2+}, Fe^{3+} & Fe^{2+} metal ion. *J. molstruc*. 1195, 670-680. https://doi.org/10.1016/j.molstruc.2019.05.088.

[2] Zhang, L., RongChen, X., Wen, S.H., Liang, R.P., Qiu, J.D. (**2019**) Optical sensors for inorganic arsenic detection. TrAC. *Trends in Analytical Chem*. 118, 869-879. https://doi.org/. 10.1016/j.trac.2019.07.013.

[3] Kaur, B., Kaur, N., Kumar, S. (**2018**) Colorimetric metal ion sensors – A comprehensive review of the years 2011–2016. *Coord Chem Rev*. 358, 13-69. https://doi.org/10.1016/j. ccr.2017.12.002

[4] Botz, M.M., Mudde, T. I. (**2000**) Modeling of natural cyanide attenuation in tailings in tailings impoundments, *Mining, Metallurgy. Exploration*. 17, 228-233. https://doi.org/10.1007 /BF03403239.

[5] Fang, G., Meng, S., Zhang, G., Pan, J. (**2001**) Spectrophotometric determination of lead in foods with dibromo-p-methyl-bromosulfonazo. *Talanta*. 54, 585-589. https://doi.org/10.1016/S0039-9140(00)00677-9.

[6] Liu, Q., Liu, T., Fang, Y. (**2020**) Perylene bisimide derivative-based Fluorescent film sensors: From sensory materials to device fabrication. *Langmuir*. 36, 2155-2169. https://doi.org/10.1021/acs.langmuir.9b03919.

[7] Matsui, H., Morimoto, M., Horimoto, K., Nishimura, Y. (**2007**) Some characteristics of fluoride-induced cell death in rat thymocytes. *J. tiv*. 21, 1113-1120. https://doi.org/10.1016/ j.tiv.2007.04.006.

[8] Gaggelli, E., Kozlowski, H., Valensin, D., Valensin, G. **(2006**) Copper Homeostasis and Neuro degenerative Disorders (Alzheimer's, Prion, and Parkinson's Diseases and Amyotrophic Sclerosis). *Chem Rev*. 106, 1995-2044. https://doi.org/10.1021/cr040410w.

[9] Strausak, D., Mercer, J.F.B., Dieter, H.H., Stremmel, W., Multhaup, G. (**2001**) Copper in disorders with neurological symptoms: Alzheimer's, Menkes, and Wilson diseases. *Brain. Res. Bull*. 55, 175-185. https://doi.org/10.1016/S0361-9230 (01)00454-3.

[10] Jaishankar, M., Tseten ,T., Anbalagan, N., Mathew, B.B., Beeregowda, K.N. (**2014**) Toxicity, mechanism and health effects of some heavy metals. *Interdiscip. Toxicol*. 7, 60-72. https://dx.doi.org/ 10.2478/intox-2014-0009.

[11] Ahamed, M., Verma, S., Kumar, A., Siddiqui., M.K.J. (**2005**) Environmental exposure to lead and its correlation with biochemical indices in children. *Sci Total Environ*. 346, 48–55. https://doi.org/10.1016/j.scitotenv.2004.12.019.

[12] Luo, X., Han, Y., Chen, X., Tang, W., Yue, T., Li, Z. (**2020**) Carbon dots derived fluorescent nanosensors as versatile tools for food quality and safety assessment: A review. *Trends Food Sci Tech*. 95, 149-161. https://doi.org/10.1016/j.tifs.2019.11.017.

[13] Shamsipur, M., Barati, A., Nematifar, Z. (**2019**) Fluorescent pH nanosensors: Design strategies and applications. *J. Photochem Photobiol Rev*. 39, 76-141. https://doi.org/10.1016/j.jphotochemrev.2019.03.001

[14] Bhalla, P., Goel, A., Tomer, N., Malhotra, R. (**2022**) Multi responsive chemosensor for the determination of metal ions (Co^{2+}, Cu^{2+}, and Zn^{2+} ions). Inorg. Chem. Commun. 136, 109181. https://doi.org/10.1016/j.inoche.2021.109181.

[15] Diana, R., Caruso, U., Di Costanzo, L., Gentile, F.S., Panunzi, B. (**2021**) Colorimetric recognition of multiple first-row transition metals: A single water-soluble chemosensor in acidic and basic conditions. *Dyes Pigments*. 184, 108832. https://doi.org/10.1016/j.dyepig.2020.108832.

[16] Li,S., He,J., Xu,Q.H. (**2020**) Aggregation of Metal-Nanoparticle-Induced Fluorescence enhancement and its Application in Sensing. *ACS Omega*. 5, 41-48. https://doi.org/10.1021/acsomega.9b03560.

[17] Andersen, C.M., Mortensen, G. (**2008**) Fluorescence Spectroscopy: A rapid tool for analyzing dairy products. *J. Agr Food Chem*. 56,720-729. https://doi.org/10.1021/jf072025o.

[18] Gowri, A., Kathiravan, A. (**2020**) Fluorescent chemosensor for detection of water pollutants, *Sen. in water Pollut. Moni*. 147-160. https://doi.org/10.1007/978-981-15- 0671-09

[19] Udhayakumari, D. (**2018**) Chromogenic and fluorogenic chemosensors for lethal cyanide ion: A comprehensive review of the year 2016. *Sensor Actuat B-Chem*. 259, 1022–1057. https://doi.org/10.1016/j.snb.2017.12.006.

[20] Channa, A.M., Siyal, A.N., Memon, S.Q., Parveen, S. (**2016**) Design of experiment for treatment of arsenic-contaminated water using Schiff's base metal complex modified Amberlite XAD-2. *Desalin & Water Treat*. 57, 3664-3673. https://doi.org/10.1080/19443994.2014.988658.

[21] Soomro, F.K., Memon, S.Q., Memon, N., Khuhawar, M. Y. (**2020**) A new Schiff's base polymer for remediation of phenol, 2-chlorophenol and 2,4-dichlorophenol from contaminated aqueous systems. *Polym Bull*. 77, 2367–2383. https://doi.org/10.1007/s00289-019-02852-6.

[22] Antony, R., Arun, T., David S.T., Manickam. (**2019**) A review on applications of chitosan-based Schiff bases. *Inter J. Bio Macro*. 129, 615-633. https://doi.org/10.1016/j.ijbiomac. 2019.02.047.

[23] Kaczmarek, M.T., Zabiszak, M., Nowak, M., Jastrzab, R. (**2018**) Lanthanides: Schiff base complexes, applications in cancer diagnosis, therapy, and antibacterial activity. *Coord. Chem Rev.* 370, 42-54. https://doi.org/10.1016/j.ccr.2018.05.012.

[24] Das, P., Linert, W. (**2016**) Schiff base-derived homogeneous and heterogeneous palladium catalysts for the Suzuki–Miyaura reaction. *Coord Chem Rev*. 31,11-23. https://doi.org/10.1016/j.ccr.2015.11.010.

[25] Udhayakumari, D., Naha, S., Velmathi, S. (**2017**) Colorimetric and fluorescent chemosensors for Cu^{2+}. A comprehensive review from the years 2013–15. J. *Anal Methods*.9, 552–578. https://doi.org/10.1039/C6AY02416E.

[26] Chen, S.Y., Li, Z., Li, K., Yu, X.Q.: Small molecular fluorescent probes for the detection of lead, cadmium and mercury ions. CoordChem Rev. 429, 213691(2021). https://doi.org/10.1016/j.ccr.2020.213691.

[27] Upadhyay, S., Singh, A., Sinha, R., Omer, S., Negi, K. (**2019**) Colorimetric chemosensors for d- metalions: A review in the past, present and future prospect. *J .Molstruc*. 1193, 89-102. https://doi.org/10.1016/j.molstruc.2019.05.007.

[28] Udhayakumari, D., Inbaraj, V. (**2020**) A Review on Schiff Base Fluorescent Chemosensors for Cell Imaging Applications. *J. Fluorescence*. 1-21. https://doi.org/10.1007/s10895-020- 02570-7.

[29] Khan, S., Chen, X., Almahri, A., Allehyani, E.S., Alhumaydhi, F.A., Ibrahim, M.M., Ali, S. (**2021**) Recent developments in fluorescent and colorimetric chemosensors based on Schiff bases for metallic cations detection: A review. *J. Environ Chemical Engg*. 9, 106381. https://doi.org/10.1016/j.jece.2021.106381.

[30] VinothKumar, G.G., Kesavan, M.P., Sivaraman, G., Rajesh, J. (**2018**) Colorimetric and NIR fluorescence receptors for F^- ion detection in aqueous condition and its Live cell imaging. *Sensor Actuat B-Chem*. 255, 3194–3206. https://doi.org/10.1016/j.snb.2017.09.145.

[31] Udhayakumari, D. (**2020**) Detection of toxic fluoride ion via chromogenic and fluorogenic sensing. A comprehensive review of the year 2015–2019. *Spectrochimca Acta A.* 228, 117817. https://doi.org/10.1016/j.saa.2019.117817.

[32] Saini, N., Prigyai, N., Wannasiri, C., Ervithayasuporn, V., Kiatkamjornwong, S. (**2018**) Green synthesis of fluorescent N,O- chelating hydrazone Schiff base for multi-analyte sensing in Cu^{2+}, F^- and CN^- ions. *J. Photochem Photobiol*. 358, 215–225. https://doi.org/10.1016/j.jphotochem.2018.03.018.

[33] Dalapati, S., Jana, S., Guchhait, N. (**2014**) Anion recognition by simple chromogenic and chromo-fluorogenic salicylidene Schiff base or reduced-Schiff base receptors. *Spectrochim Acta A*. 129, 499-508. https://doi.org/10.1016/j.saa.2014.03.090.

[34] Udhayakumari, D., Velmathi, S., Chen, W.C., Wu, S. P. (**2014**) A dual-mode chemosensor: Highly selective colorimetric fluorescent probe for Cu^{2+} and F^- ions. *Sensor Actuat B-Chem*. 204, 375-381. https://doi.org/10.1016/j.snb.2014.07.109.

[35] Bhuvanesh, N., Suresh, S., Prabhu, J., Kannan, K., Rajesh Kannan, V., Nandhakumar, R. (**2018**) Ratiometric fluorescent chemosensor for silver ion and its bacterial cell imaging. Opt *Mat*. 82, 123–129. https://doi.org/10.1016/j.optmat.2018.05.053.

[36] Kolcu, F., Erdener, D., Kaya, I. (**2020**) A Schiff base based on triphenylamine and thiophene moieties as a fluorescent sensor for Cr (III) ions: Synthesis, characterization and fluorescent applications. *Inorganica Chimica Acta*. 509, 119676. https://doi.org/10.1016/j.ica.2020.119676.

[37] Chalmardi, G.B., Tajbakhsh, M., Hasani, N., Bekhradnia, A. (**2018**) A new Schiff-base as fluorescent chemosensor for selective detection of Cr^{3+}: An experimental and theoretical study. *Tetrahedron*. 74, 2251-2260. https://doi.org/10.1016/j.tet.2018.03.046.

[38] Zhang, M., Gong, L., Sun, C., Li, W., Chang, Z., Qi, D. (**2019**) A new fluorescent-colorimetric chemosensor based on a Schiff base for detecting Cr^{3+}, Cu^{2+}, Fe^{3+} and Al^{3+} ions. *Spectrochimica Acta Part A*. 214, 7-13. https://doi.org/10.1016/j.saa.2019.01.089.

[39] Vijayakumar, P., Dhineshkumar, E., Doss, M.A., Negar, S.N., Renganathan, R. (**2021**) Novelschiff base synthesis of E-N-(1-(1H-phenothiazin-2yl)-ethylidene)-3-((E)-(2-phenyl hydrzono) methyl) aniline ‘‘Turn-on”fluorescent chemosensor for sensitivity and selectivity of detetion of Cr^{3+} and Pb^{2+} ions. *Mat Today: Pro*. 42, 1050-1064. https://doi.org/10.1016/j.matpr.2020.12.124.

[40] Chandra, R., Manna, A.K., Sahu, M., Rout, K., Patra, G.K. (**2020**) Simple salicylaldimine functionalized dipodal bis Schiff base chromogenic and fluorogenic chemosensors for selective and sensitive detection of Al^{3+} and Cr^{3+}. *Inorganica Chimica Acta*. 499, 119192. https://doi.org/10.1016/j.ica.2019.119192.

[41] Dhineshkumar, E., Iyappan, M., Anbuselvan, C. (**2020**) A novel dual chemosensor for selective heavy metal ions Al^{3+}, Cr^{3+} and its applicable cytotoxic activity, HepG2 living cell images and theoretical studies. *J .molstruc*. 15, 1128033. https://doi.org/10.1016/ j.molstruc.2020.128033.

[42] Hu, T., Wang, L., Li, J., Zhao, Y., Cheng, J., Li, W., Chang, Z., Sun, C. (**2021**) A new fluorescent sensor L based on fluorene-naphthalene Schiff base for recognition of Al^{3+} and Cr^{3+}. *Inorganica Chimica Acta*. 524, 120421. https://doi.org/10.1016/j.ica.2021.120421.

[43] Mukherjee, S., Betal, S., Chattopadhyay, A.P. (**2020**) Dual sensing and synchronous fluorescence spectroscopic monitoring of $Cr^{3+}$and Al^{3+} using a luminescent Schiff base: Extraction and DFT studies. *Spectrochimica Acta Part A: Mole and Biomole Spec*. 228, 117837. https://doi.org/10.1016/j.saa.2019.117837.

[44] Mahata, S., Janani, G., Mandal, B.B., Manivannan, V. (**2021**) A coumarin based visual and fluorometric probe for selective detection of Al(III), Cr(III) and Fe(III) ions through “turn-on” response and its biological application. *J Photochem and Photobio A: Chem*. 417, 13340. https://doi.org/10.1016/j.jphotochem.2021.113340.

[45] Singh,G., Sindhu, J., Manisha, Kumar, V., Sharma, V., Sharma, S.K., Mehta, S.K., M.H., Umar, A., Kataria, R. (**2019**) Development of an off-on selective fluorescent sensor for the detection of Fe^{3+} ions based on Schiff base and its Hirshfeld surface and DFT studies. *J. Mol Liq*. 296, 111814. https://doi.org/10.1016/j.molliq.2019.111814.

[46] Çelik, G.G., Şenkuytu, E., Şahin, O., Serin, S. (**2021**). The new water-soluble Schiff base derivative fluorometric chemosensor with highly selective and instantly sensitivity for Fe^{3+} ion detection in aqueous media. *Inorganica Chimica Acta*. 527, 120556. https://doi.org/10.1016/ j.ica.2021.120556.

[47] Yang, Y.S., Liang, C., Yang, C., Zhang, Y.P., Wang, .B.X., Liu, J. (**2020**) A novel coumarin-derived acylhydrazone Schiff base gelator for synthesis of organogels and identification of Fe^{3+}. *Spectrochimica Acta Part A*. 237, 118391. https://doi.org/10.1016/j.saa.2020.118391.

[48] Sawminathan, S., Munusamy, S., Manickam, S., Jothi, D., KulathuIyer, S. (**2021**) Azine based fluorescent rapid "off-on" chemosensor for detecting Th^{4+} and Fe^{3+} ions and its real-time application. *Dyes and Pig*. 196, 109755. https://doi.org/10.1016/j.dyepig.2021.109755.

[49] Yin, Z.Y., Hu, J.H., Gui, K., Fu, Q.Q., Yao, Y., Zhou, F.L., Ma, L.L., Zhang, Z.P. (**2020**) AIE based colorimetric and “turn-on” fluorescence Schiff base sensor for detecting Fe^{3+} in an aqueous media and its application. *J. Photochem Photobio A. Chem*. 396, 112542. https://doi.org/10.1016/j.jphotochem.2020.112542.

[50] Gong, X.., Ding, X., Iang, N.J., Zhong, T., Wang, G. (**2020**) Benzothiazole-based fluorescence chemosensors for rapid recognition and “turn-off” fluorescence detection of Fe^{3+} ions in aqueous solution and in living cells. *J. Microc*. 152, 104351. https://doi.org/10.1016/j.microc.2019.104351.

[51] Özdemir, O. (**2021**) A new 2-hydroxynaphthalene based Schiff base receptor for detection of Cu^{2+}, Fe^{3+}, $HSO4^{-}$, CN^{-} ions and D–amino acids in aqueous DMSO solution. *J. Molstruc*. 1240, 130532. https://doi.org/10.1016/j.molstruc.2021.130532.

[52] He, X., Xie, Q., Fan, J., Xu, C., Xu, W., Li, Y., Ding, F., Deng, H., Chen, H., Shen, J. (**2018**) Dual-functional chemosensor with colorimetric/ratiometric response to Cu(II)/Zn(II) ions and its applications in bio imaging and molecular logic gates. *Dye pigments*. 177, 108255. https://doi.org/10.1016/j.dyepig.2020.108255.

[53] Farhi, A., Firdaus, F., Saeed, H., Mujeeb, A., Shakir, M., Owais, M. (**2019**) A quinoline-based fluorescent probe for selective detection and real-time monitoring of copper ions - a differential colorimetric approach. *Photochem. Photobiol. Sci*. 18, 3008–3015. https://doi.org/10.1039/C9PP00247B.

[54] Ye, H., Ge, F., Zhou, Y.M., Liu, J.T., Zhao, B.X. (**2013**) A new Schiff base fluorescent probe for imaging Cu^{2+} in living cells. *Spectrochimica Acta Part A: Mol and Biomol Spectro*. 112, 132-138. https://doi.org/10.1016/j.saa.2013.03.093.

[55] Liang, S., Tong, Q., Qin, X., Liao, X., Q. Li, Yan, Q. (**2020**) A hydrophilic naphthalimide-based fluorescence chemosensor for Cu^{2+} ion: Sensing properties, cell imaging and molecular logic behavior. *Spectrochim Acta A: Molecular and biomolecular Spec.* 230, 118029. https://doi.org/10.1016/j.saa.2020.118029.

[56] Ben-nan, C., Qin, H., Yan, H., Chun-man, J., Qi, Z. (**2013**) Highly sensitive and selective chemosensor for Cu $^{2+}$ based on a Schiff base. *Chem. Res. Chin. Univ*. 29, 419-423. https://doi: 10.1007/s40242-013-2449-4.

[57] Wang, X., Shi, W., Feng, L., Ma, J., Li, Y., Kong, X., Chen, Y., Hui, Y., Xie , Z. (**2017**) A highly selective and sensitive Schiff-base based turn-on optical sensor for Cu^{2+} in aqueous medium and acetonitrile. *J. Inorg chem*. 79, 50-54. https://doi.org/10.1016/j.inoche.2017.03.006.

[58] Manna, A.K., Mondal, J., Rout, K., Patra, G.K. (**2018**) A new ICT based Schiff-base chemosensor for colorimetric selective detection of copper and its copper complex for both colorimetric and fluorometric detection of Cysteine. *J Photochem and Photobio A: Chem*. 367, 74-82. https://doi.org/10.1016/j.jphotochem.2018.08.018.

[59] Sahu M., Manna, A.K., Rout, K., Mondal, J., Patra G.K. (**2020**) A highly selective thiosemicarbazone based Schiff base chemosensor forcolorimetric detection of Cu^{2+} and Ag^{+} ions and turn-on fluorometric detection of Ag^{+} ions. *Inorganica Chimica Acta*. 508, 119633. https://doi.org/10.1016/j.ica.2020.119633.

[60] Gurusamy, S., Krishnaveni, K., Sankarganesh, M., Sathish, V., Thanasekaran, P., Mathavan , A. (**2021**) Multiple target detection and binding properties of naphthalene-derived Schiff- base chemosensor. *J. Mol Liq*. 325, 115190. https://doi.org/10.1016/ j.molliq.2020.115190.

[61] Anbu, S., Paul, A., Surendranath, K., Solaiman, N.S., Pombeiro, A.J.L. (**2021**) A benzimidazole-live-cell imaging and pyrosequencing applications. *Sens Actua B: Chem*. 337, 129785. https://doi.org/10.1016/j.snb.2021.129785.

[62] Cheah, P.W., Heng, M.P., Saad, H.M., Sim, K.S., Tan, K.W. (**2021**) Specific detection of Cu^{2+} by a pH-independent colorimetric rhodamine based chemosensor. *J. Opt Mat*. 114, 110990. https://doi.org/10.1016/j.optmat.2021.110990.

[63] D. Mohanasundaram, R. Bhaskar, M. Sankarganesh, K. Nehru, G.G. Vinoth Kumar, Rajesh, J. (**2022**) A simple pyridine based fluorescent chemosensor for selective detection of copper ion. *Spectrochimical Acta Part A: Mole and Biomol Spectro*. 265, 20395. https://doi.org/10.1016/j.saa.2021.120395.

[64] Chan, W.C., Saad, H.M., Sim, K.S., Lee, V.S., Ang, C.W., Yeong, K.W., Tan, K.Y. (**2021**) A rhodamine based chemosensor for solvent dependent chromogenic sensing of cobalt (II) and copper (II) ions with good selectivity and sensitivity: Synthesis, filter paper test strip, DFT calculations and cytotoxicity. *Spectro chimical Acta Part A: Mol and Biomol Spectro*. 262, 120099. https://doi.org/10.1016/j.saa.2021.120099.

[65] Vashisht, D., Sharma, S., Kumar, R., Saini, V., Saini, V., Ibhadon, A., Sahoo, S.C., Sharma, S., Mehta, S.K., Kataria,R. (**2020**) Dehydroacetic acid derived Schiff base as selective and sensitive colorimetric chemosensor for the detection of Cu(II) ions in aqueous medium. *J. Microchem*. 155, 104705. https://doi.org/10.1016/j.microc.2020.104705.

[66] Liu, B., Tan, Y., Hu, Q., Wang, Y., Wu, X., Huang, Q., Zhang, W., Zheng, M., Wang, H. (**2019**) A naked eye fluorescent chemosensor for Zn^{2+} based on triphenylamine derivative and its bio imaging in live cells. *J. Chem Papers*. 73, 3123–3134. https://doi.org/10.1007/s11696-019-00853-3.

[67] Kumar, M., Kumar, A., Singh, M., Sahu, S. K., John, R. P. (**2017**) A novel benzidine based Schiff base "turn-on" fluorescent chemosensor for selective recognition of Zn^{2+}. *Sens and Actu B: Chem*. 241, 1218-1223. https://doi.org/10.1016/j.snb.2016.10.008.

[68] Mondal, S., Mandal, S.M., Ojha, D., Chattopadhyay, D ., Sinha, C. (**2019**) Water soluble sulfaguanidine based Schiff base as a "Turn-on" fluorescent probe for intracellular recognition of Zn^{2+} in living cells and exploration for biological activities. *Polyhedron*. 172, 28-38. https://doi.org/10.1016/j.poly.2019.02.042.

[69] Rout, K., Manna, A.K., Sahu, M., Patra, G.K. (**2019**) A guanidine based bis Schiff base chemosensor for colorimetric detection of Hg (II) and fluorescent detection of Zn (II) ions. *Inorganica Chimica Acta*. 486, 733-741. https://doi.org/10.1016/j.ica.2018.11.021.

[70] Sun, Y.X., Li, J., Guo, G., Sun, Y.G., Ding, W.M. (**2021**) Synthesis, structural characterizations and Spectroscopic properties of binuclear Co^{III} complex and its Schiff ligand as a chemosensor for fluorescent recognition of Zn^{II}. *Inorganica Chimica Acta*. 527, 120581. https://doi.org/10.1016/j.ica.2021.120581.

[71] Xue, W.Z., Han, X.F., Zhao, X.L., Wu, W.N., Wang, Y., Xu, Z.Q., Fan, Y.C., Xu, Z.H. (**2021**) An AIRE-active far-red ratiometric fluorescent chemosensor for specifically sensing Zn^{2+} and resultant Zn^{2+} complex for subsequent pyrophosphate detection in almost pure aqueous media. *Spectrochimica Acta Part A: Mol and Biomole Spectro*. 263, 120169. https://doi:10.1016/j.saa.2021.120169.

[72] Das, M., Koley, B., Das, U.K., Bag, A., Laha, S., Samanta, B.C., Choudhuri, I., Bhattacharyya, N., Maity, T. (**2021**) Piperidine based effective chemosensor for Zn (II) with the formation of binuclear Zn complex having specific Al (III) detection ability in aqueous medium and live cell images. *J. Photochem and Photobio A: Chem*. 415, 113302. https://doi 10.1016/j.jphotochem.2021.113.

[73] Maity, D., Mandal, S K., Guha, B., Roy, P. (**2021**) A salicylaldehyde based dual chemosensor for zinc and arsenate ion detection: Biological application. *Inorganica Chimica Acta*. 519, 120258. https://doi.org/10.1016/j.ica.2021.120258.

[74] Mathew, M.M., Sreekanth, A. (**2021**) Zn^{2+}ion responsive fluorescent chemosensor probe of Thiophene-diocarbohydrazide derivatives. *Inorganica Chimica Acta*. 516, 120149. https://doi.org/10.1016/j.ica.2020.120149.

[75] Park, S., Lee, H., Yi, Y., Lim, M.H., Kim, C. (**2020**) A rhodanine-based fluorescent chemosensor for sensing Zn^{2+} and Cd^{2+}: Applications to water sample and cell imaging. *Inorganica Chimica Acta*. 513, 119936. https://doi.org/10.1016/j.ica.2020.119936.

[76] Cheng, T., Xu, Y., Zhang, S., Zhu, W., Qian, X., Duan, L. (**2008**) A Highly Sensitive and Selective OFF - ON Fluorescent Sensor for Cadmium in Aqueous Solution and Living Cell. *J. Am. Chem. Soc.* 130, 16160-16161. https://doi.org/10.1021/ja806928n.

[77] Zhao, Q., Li, R.F., Xing, S.K., Liu, X.M., Hu, T.L., Bu, X.H. (**2011**) A Highly Selective On/Off Fluorescence Sensor for Cadmium (II). *Inorg Chem*. 50, 10041-10046. https://doi.org/10.1021/ic2008182.

[78] Soibinet, M., Souchon, M., Leray, I., Valeur, B. (**2008**) Rhod-5N as a Fluorescent Molecular Sensor of Cadmium (II) Ion. *J Fluoresc*. 18(6), 1077. https://doi.org/10.1007/s10895-008-0352-z.

[79] Li, S., Lu, L., Zhu, M., Yuan, C., Feng, S. (**2018**) A bifunctional chemosensor for detection of volatile ketone or hexavalent chromate anions in aqueous solution based on a Cd (II) metal–organic frame work. *Sens ActuaB: Chem*. 258, 970-980. https://doi.org/10.1016/j.snb.2017.11.142.

[80] Yan, J., Fan, L., Qin, J.C., Li, C.R., Yang, Z.Y. (**2016**) A novel chromone Schiff-base fluorescent chemosensor for Cd(II) based on C=N isomerization. *J. Fluoresc*. 26, 1059-10651. https://doi.org/10.1007/s10895-016-1794-3.

[81] Wan, X., Ke, H., Tang, J., Yang, G. (**2019**) Acid Environment-improved fluorescence sensing performance: A quinoline Schiff base-containing sensor for Cd^{2+} with high sensitivity and selectivity. *Talanta*. 199, 8-13. https://doi.org/10.1016/j.talanta.2019.01.101.

[82] Liu, Y., Qiao, Q., Zhao, M., Yin, W., Miao, L., Wang, L. Z. Xu, L. (**2016**) Cd^{2+}-triggered amide tautomerization produces a highly Cd^{2+}-selective fluorescent sensor across a wide pH range. *Dyes Pigments*. 133, 339-344. https://doi.org/10.1016/j.dyepig.2016.06.017.

[83] Mohanasundaram, D., Bhaskar, R., Vinoth Kumar, G.G., Rajesh, J., Rajagopal, G. (**2021**) A quinoline based Schiff base as a turn-on fluorescence chemosensor for selective and robust detection of Cd^{2+} ion in semi-aqueous medium. *J. Microc*. 106030. https://doi.org/10.1016/j.microc.2021.106030.

[84] Khan, SA., Ullah, Q., Almalki, A.S.A., Kumar, S., Obaid, RJ., Alsharif, MA., Alfaifi, SY., Hashmi, AA. (**2021**) Synthesis and photophysical investigation of (BTHN) Schiff base as off- on Cd^{2+} fluorescent chemosensor and its live cell imaging. *J. Mol. Liq*. 328, 115407. https://doi.org/10.1016/j.molliq.2021.115407.

[85] Chen, W., Xu, H., Ju, L., Lu, H. (**2021**) A highly sensitive fluorogenic "turn-on" chemosensor for the recognition of Cd^{2+} based on a hybrid purine-quinoline Schiff base. *Tetrahedron*. 88, 132123. https://doi.org/10.1016/j.tet.2021.132123.

[86] Rha, CJ., Lee, H., Kim, C. (**2020**) An effective phthalazine-imidazole-based chemosensor for detecting Cu^{2+}, Co^{2+} and S^{2-} via the color change. *Inorganica Chimica Acta*. 511, 119788. https://doi.org/10.1016/j.ica.2020.119788.

[87] Kim, PA., Lee, H., So, H., Kim, C. (*2020*) A chelated-type colorimetric chemosensor for sensing Co^{2+} and Cu^{2+}. *Inorganica. Chimica. Acta*. 505, 119502. https://doi.org/10.1016/j.ica.2020.119502.

[88] Pungut, N.A., Heng, M.P., Saad, H.M., Sim, K.S., Lee, V.S., Tan, K.W. (**2021**) From one to three, modifications of sensing behavior with solvent system: DFT calculations and real-life application in detection of multianalytes (Cu^{2+}, Ni^{2+} and Co^{2+}) based on a colorimetric Schiff base probe. *J. Molstruc*. 1238, 130453. https://doi.org/10.1016/j.molstruc.2021.130453.

[89] Alamgir, S., Rhaman, M.M., Basaran, I., Powell, D.R., Hossain, M.A. (**2020**) Colorimetric and spectroscopic cobalt (II) sensing by a simple Schiff base. *J Poly*. 187, 114681. https://doi.org/10.1016/j.poly.2020.114681.

[90] Rani, B.K., John, S.A. (**2018**) Fluorogenic mercury ion sensor based on pyrene-amino mercapto thiadiazole unit. *J. hazard mat*. 343, 98-106. https://doi.org/10.1016/j.jhazmat .2017.09.028.

[91] Wu, Y., Wen, X., Fan, Z. (**2019**) An AIE active pyrene based fluorescent probe for selective sensing Hg^{2+} and imaging in live cells. *Spectrochim Acta A: Mol and biomol spectro*. 223, 117315. https://doi.org/10.1016/j.saa.2019.117315.

[92] Musikavanhu, B., Muthusamy, S., Zhu, D., Xue, Z., Yu, Q., Chiyumba, C.N., Mack, J., Nyokong, T., Wang, S., Zhao, L. (**2022**) A simple quinoline-thiophene Schiff base turn-off chemosensor for Hg^{2+} detection: spectroscopy, sensing properties and applications. *Spectrochimica Acta Part A: Mol and Biomol Spectro*. 264, 120338. https://doi.org/10.1016/j.saa.2021.120338.

[93] Huang, L., Sheng, W., Wang, L., Meng, X., Duan, H., Ch, L. (**2021**) A novel coumarin-based colorimetric and fluorescent probe for detecting increasing concentrations of Hg^{2+} in vitro and in vivo. *RSC Adv*. 11, 23597-23606. https://doi.org/10.1039/D1RA01408K.